Natural Resources Canada | Ressources naturelles Canada

GEOLOGICAL SURVEY OF CANADA
OPEN FILE 8823

Geochemical data for stream and groundwaters around the Casino Cu-Au-Mo porphyry deposit, Yukon (NTS 115 J/10 and 115 J/15)

J.A. Kidder, M.B. McClenaghan, M.I. Leybourne, M.W. McCurdy, P. Pelchat, D. Layton-Matthews, C.E. Beckett-Brown, and A. Voinot

2022

Canada

GEOLOGICAL SURVEY OF CANADA
OPEN FILE 8823

Geochemical data for stream and groundwaters around the Casino Cu-Au-Mo porphyry deposit, Yukon (NTS 115 J/10 and 115 J/15)

J.A. Kidder[1], M.B. McClenaghan[1], M.I. Leybourne[2,3], M.W. McCurdy[1], P. Pelchat[1], D. Layton-Matthews[2], C.E. Beckett-Brown[4], and A. Voinot[2,3]

[1]Geological Survey of Canada, 601 Booth Street, Ottawa, Ontario
[2]Queens's Facility for Isotope Research, Department of Geological Sciences and Geological Engineering, Queen's University, 36 Union Street, Kingston, Ontario
[3]Arthur B. McDonald Canadian Astroparticle Physics Research Institute, Department of Physics, Engineering Physics and Astronomy, Queen's University, 64 Bader Lane, Kingston, Ontario
[4]Harquail School of Earth Sciences, Laurentian University, 935 Ramsey Lake Road, Sudbury, Ontario

2022

Permanent link: https://doi.org/10.4095/328862

This publication is available for free download through GEOSCAN (https://geoscan.nrcan.gc.ca/).

Recommended citation

Kidder, J.A., McClenaghan, M.B., Leybourne, M.I., McCurdy, M.W., Pelchat, P., Layton-Matthews, D., Beckett-Brown, C.E., and Voinot, A., 2022. Geochemical data for stream and groundwaters around the Casino Cu-Au-Mo porphyry deposit, Yukon (NTS 115 J/10 and 115 J/15); Geological Survey of Canada, Open File 8823, 1 .zip file. https://doi.org/10.4095/328862

Publications in this series have not been edited; they are released as submitted by the author

Table of Contents

Appendix B2 Stream water isotopic data *(digital data file)*

Appendix C1 Proportional dot maps of geochemical data for stream waters. Bedrock geology from Yukon Geological Survey (2018b). *(digital data files)*

Bedrock geology legend
Map 1 Stream water and groundwater sample locations
Map 2 pH
Map 3 Conductivity
Map 4 Fe
Map 5 Mn
Map 6 Ca
Map 7 NO_3
Map 8 SO_4^{2-} and $\delta^{34}S$
Map 9 Cu
Map 10 Mo
Map 11 Pb
Map 12 Zn
Map 13 Cd
Map 14 Co
Map 15 Re
Map 16 U

LIST OF TABLES

LIST OF FIGURES

sites (red stars). Sample numbers are shown in black beside each sample site. Bedrock geology from Yukon geological Survey (2020k, m). Location of mineral occurrences from Yukon Geological Survey (2020f, e, k, m, g, j, b, i, l, a, h).

Figure 3. Copper (ppb) in stream water samples collected around the Casino deposit in 1969 (modified from Archer and Main, 1971).

Figure 4. Modified Piper plot of ground and surface waters from the Casino deposit area. A) cations, and B) anions. Waters closest to the Casino deposit have proportionally higher SO_4^{2-} and Ca concentrations and the highest TDS.

Figure 5. Plots of major ions and Fe, F versus total dissolved solids (TDS) for Casino surface and groundwaters.

Figure 6. A) Plots of trace elements (B, U, F, Sr, and Zn) and pH versus SO_4^{2-} concentrations for Casino surface and groundwaters., and B) Plots of trace elements (Fe, Mn, Cu, Mo, As, and Re) versus SO_4^{2-} concentrations for Casino surface and groundwaters.

Figure 7. A) Cl- chondrite-normalized rare earth element patters (McDonough and Sun, 1995), and B) Ce anomaly (Ce*) versus Mn concentrations for ground and surface waters from the Casino area. NASC normalizing values from (McLennan, 1989).

Figure 8. Oxygen and hydrogen isotopic composition of Casino surface and groundwaters, including the Global Meteoric Water Line (GMWL) (Craig, 1961). A) Also included are monthly weighted averages for precipitation at monitoring stations at Mayo and Whitehorse, Yukon. Data from IAEA/WMO (2019). Global Network of Isotopes in Precipitation. The GNIP Database. Accessible at: https://nucleus.iaea.org/wiser. B) Expanded view of Casino waters and the GMWL.

Figure 9. $\delta^{34}S$ versus SO_4^{2-} concentrations for dissolved sulfate in Casino surface and groundwaters.

Figure 10. Strontium isotope ratios in Casino surface and groundwaters compared to A) Rb/Sr; B) Na/Cl; C) Cu; and D) Mo.

Figure 11. A conceptual model with east-west section with deposit mineralogy, host geology and hydrology.

Figure 12. Metals and metalloids versus Re concentrations for Casino surface and groundwaters.

ABSTRACT

This open file reports geochemical data for stream and groundwater samples collected around the Casino porphyry Cu-Au-Mo deposit, one of the largest and highest-grade deposits of its kind in Canada. The calc-alkaline porphyry is hosted in a Late Cretaceous quartz monzonite and associated breccias in the unglaciated region of west central Yukon. Water chemistry around the deposit was investigated because: (i) the deposit has not yet been disturbed by mining; (ii) the deposit was known to have metal-rich waters in local streams; and (iii) the deposit has atypically preserved ore zones. Stream water samples were collected at 22 sites and groundwater samples were collected from eight sites. Surface and groundwaters around the Casino deposit are anomalous with respect to Cd (up to 5.4 µg/L), Co (up to 64 µg/L), Cu (up to 1657 µg/L), Mo (up to 25 µg/L), As (up to 17 µg/L), Re (up to 0.7 µg/L), and Zn (up to 354 µg/L) concentrations. The stable isotopes of O and H of the groundwaters are essentially identical to the surface waters and plot close to the local and global meteoric water lines, indicating that the waters represent modern recharge, consistent with the generally low salinities of all the waters (total dissolved solids range from 98 to 1320 mg/L). Sulfur and Sr isotopes are consistent with proximal waters interacting with the Casino rocks and mineralization; a sulfide-rich bedrock sample from the deposit has $\delta^{34}S$ = -1.2 ‰ and proximal groundwaters are only slightly heavier (-0.3 to 3.1 ‰). These geochemical and isotopic results indicate that surface water geochemistry is a suitable medium for mineral exploration for porphyry-style mineralization in the Yukon, and similar unglaciated regions in Canada. The atypical geochemical signature (Mo, Se, Re, As, Cu) of these types of deposits are typically reflected in the water chemistry and S isotopes provide a more local vectoring tool.

INTRODUCTION

Because much of Canada is covered in glacial sediments, surficial geochemical tools including till geochemistry and indicator minerals are commonly used to discover buried mineralization at or near the bedrock interface (McClenaghan, 2005; Thorleifson, 2017; McClenaghan and Paulen, 2018). However, where potential mineralization is at significantly greater depth and thus unaffected by glacial transport, or in rare parts of Canada that were not affected by the last glaciation, other geochemical exploration methods can be useful. The use of groundwater as a sample medium in Canadian mineral exploration has a long history (Boyle, 1978; Cameron, 1978; Leybourne et al., 2003; McClenaghan et al., 2015), however, it is only in the last two decades that analytical technologies with sufficiently low detection limits have become widespread, in particular in commercial laboratories (Leybourne, 2007; Leybourne and Cameron, 2010; Buskard et al., 2020). More recently, emphasis has been placed on the use of isotopic techniques to assist in the interpretation of aqueous geochemical data or to provide direct vectors to

mineralization (Leybourne and Cousens, 2005; Mathur et al., 2005; Leybourne and Cameron, 2006a; Leybourne et al., 2006; Leybourne et al., 2009; Mathur et al., 2012; Mathur et al., 2013; and Skierszkan et al., 2019; Kidder et al., 2021).

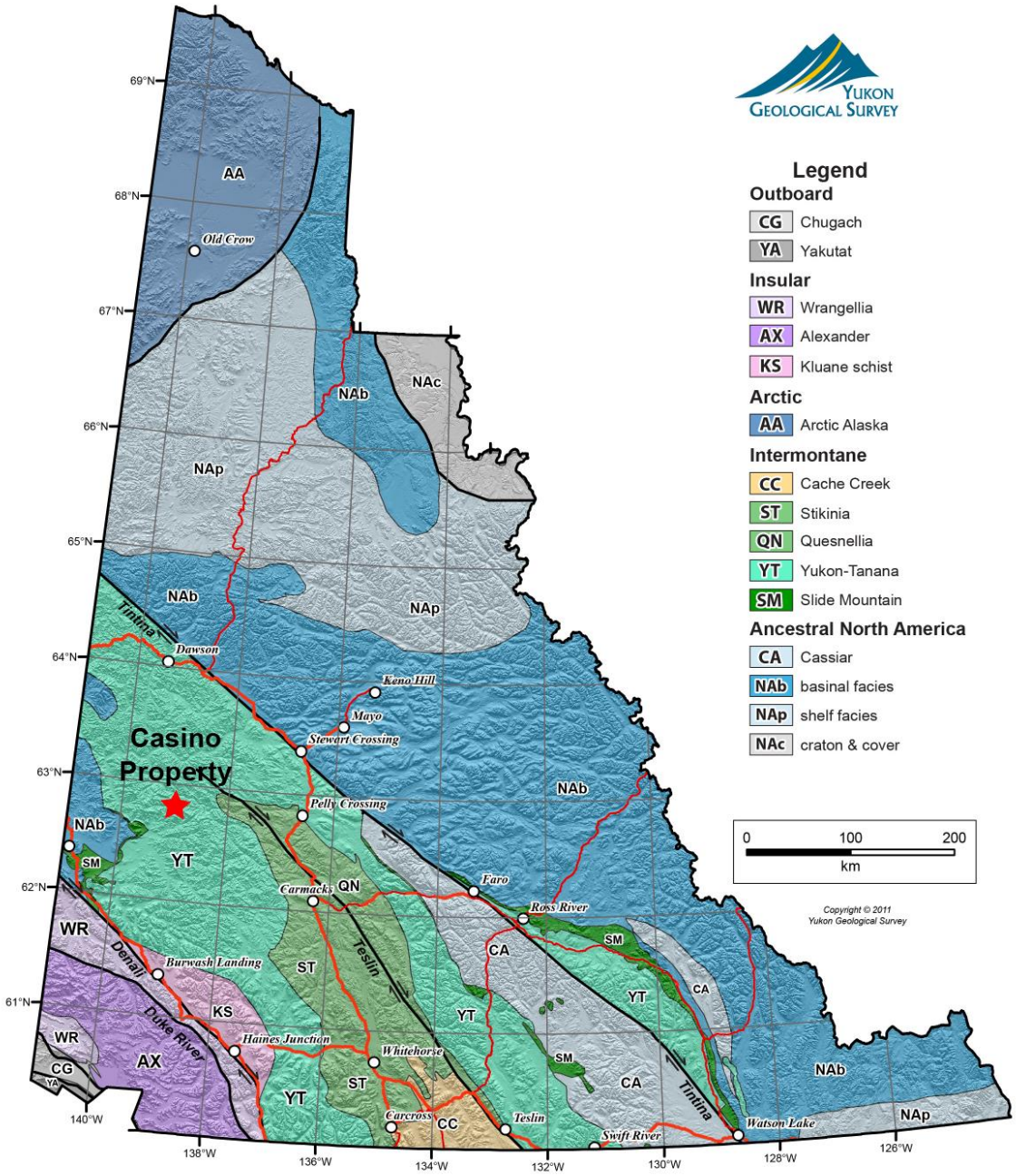

Figure 1. *Location of the Casino porphyry Cu deposit in west central Yukon (modified from Relf (2020).*

The Casino deposit in the west-central Yukon is one of Canada's largest and highest-grade porphyry Cu-Au-Mo deposits (Roth et al., 2020). It provides an ideal site for testing

modern stream water and groundwater geochemical methods because the deposit has only been minimally disturbed by exploration (not yet mined) and is known to have metal-rich waters and sediments in creeks draining the deposit (Archer and Main, 1971).

A stream sediment and water study were carried out around the deposit in 2017 as part of a larger Geological Survey of Canada (GSC) study of the indicator mineral and surficial geochemical signatures of this very large deposit (McClenaghan et al., 2018; McCurdy et al., 2019; Beckett-Brown et al., 2019; McClenaghan et al., 2019; McClenaghan et al., 2020). The purpose of this open file is to report Casino stream and groundwater geochemical data for samples collected by the GSC and Western Copper and Gold Corporation. The objectives include the identification of hydromorphic dispersion of elements from the ore body along with the fractionation of isotopes resulting from geochemical reactions and identify the validity of hydrogeochemistry as a contaminant source tracer and vector for mineral exploration and environmental studies.

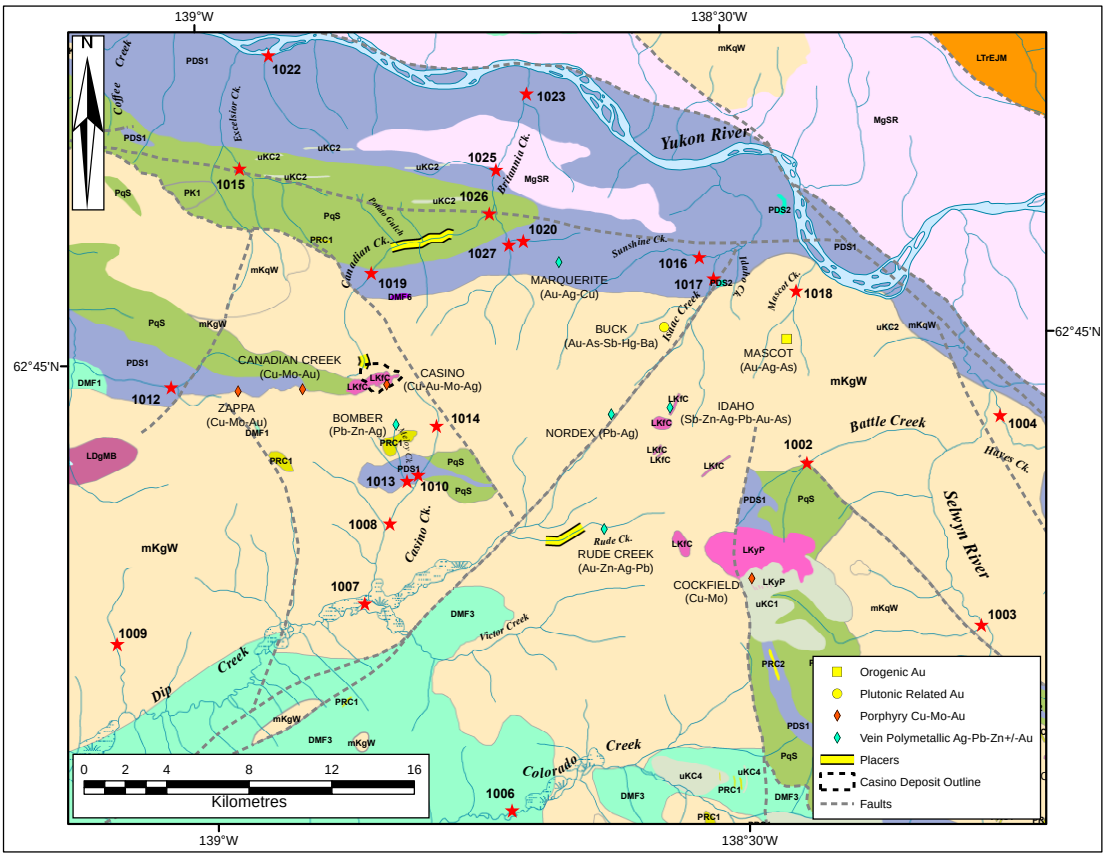

Figure 2a. *Local bedrock geology of the Casino deposit area, location of mineral occurrences in the Casino area, and location of heavy mineral stream sediment sample sites (red stars). Sample numbers are shown in black beside each sample site. Bedrock geology from Yukon geological Survey (2020k, m). Location of mineral occurrences from Yukon Geological Survey (2020 f, e, k, m, g, j, b, i, l, a, h).*

The earliest exploration in the Casino area was for placer gold (Fig. 2) in the lower reaches of Canadian Creek in 1911 (Bostock, 1959). Further upstream, a gold-tungsten placer at the junction of Canadian Creek and Patton Gulch on the northwest flank of the deposit was first worked to mine the tungsten in 1916. When the upper placer was worked again in the 1940s, the following minerals were recovered from the black sand: ferberite, gold, magnetite, hematite, scheelite, molybdenum, zircon, cassiterite, tourmaline and titanite (Bostock, 1959; Archer and Main, 1971). Over the years, placer gold mining also occurred on Rude Creek (Fig. 2), southeast of the Casino deposit (Chapman et al., 2014). Other early exploration in the Casino area focused on the silver-lead-zinc veins at the Bomber occurrence (Yukon Geological Survey, 2020e) on the south periphery of what is now known as the Casino deposit (Fig. 2).

Figure 2b. Bedrock geology map legend (Yukon geological Survey, 2020k, m).

Prior to the initial diamond drilling that resulted in discovery of the Casino deposit, surface indications of the presence of the deposit included: the prominent (730 m long) limonite gossan along a small creek on southeast side of the deposit that empties into upper Casino Creek; the presence of the local gold-tungsten placer; intense hydrothermal alteration and presence of limonite, jarosite and weak malachite staining in leached rocks at the surface; the peripheral silver-zinc-lead veins; and anomalous Cu concentrations in -80 mesh stream silt samples in Casino Creek as compared to values for the Dawson Range compiled over several years by Archer and Main (1971). Anomalous contents of Cu and Mo in -80 mesh soil samples collected in 1968 were used to guide the exploration drilling in 1969 that led to the discovery of Cu-Au mineralization (Archer and Main, 1971). Current total measured and indicated resources of the deposit are 2.173 billion tonnes grading 0.16% Cu, 0.18 g/t Au, 0.17% Mo, and 1.4 g/t Ag (Western Copper and Gold Corporation, 2020).

Archer and Main (1971) reported that the Casino deposit had an obvious geochemical signature in stream sediments (Cu, Mo, Au and Ag) and waters (Fig. 3; Cu) overlying the deposit at the time of its discovery. Subsequent reconnaissance-scale stream water and sediment sampling in NTS map sheets 115J and 115K by the GSC (pH, F, U in water; 19 elements in <0.177 mm stream sediment, Geological Survey of Canada, 1987) showed that a multi-element geochemical anomaly (Ag, Cu, Mo, Pb, Sb, W) is obvious in the local creeks draining the Casino deposit.

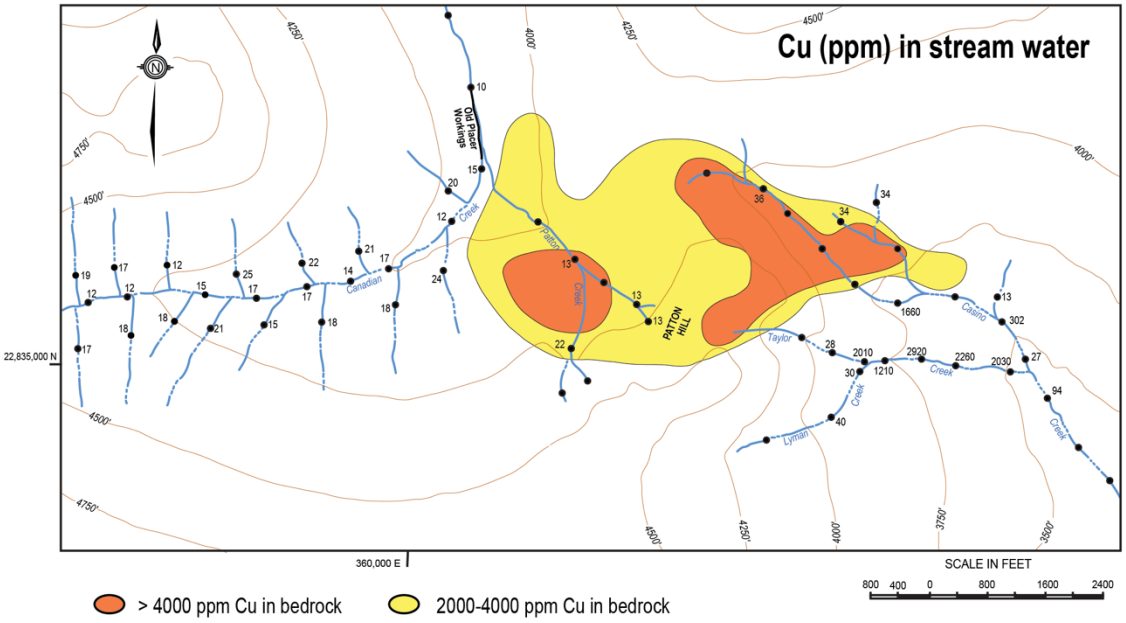

Figure 3. Copper (ppb) in stream water samples collected around the Casino deposit in 1969 (modified from Archer and Main, 1971).

PHYSIOGRAPHIC, CLIMATIC AND GEOLOGIC SETTING

Location and access

The study area is in west-central Yukon, 300 km north-west of Whitehorse (Fig. 1) and within the Klondike Plateau ecoregion (Smith et al., 2004). The deposit is located at latitude 62°44'N and longitude 138°50'W, in NTS map areas 115J J/010 (Colorado Creek) and 115J J/15 (Britannia Creek) and is accessed by fixed wing aircraft or helicopter. Creeks draining the northwest side of the deposit flow northward and eventually into the Yukon River which flows northwest. Most of the terrain lies at elevations of 1000-1500 m asl. The climate of the study area is cold and semi-arid (Bond et al., 2010) with a mean annual temperature of approximately -5.5°C: the mean annual summer temperature is 10.5°C and the winter mean annual temperature is -23°C. The mean annual precipitation ranges from 300 to 450 mm (Smith et al., 2004). The deposit is in the Dawson Range, a series of broad ridges and summits that vary in elevation from about 1000 to 1800 m asl. The highest peaks in the study area are an unnamed peak (1672 m asl) 3 km to the northwest of Patton Hill (highest point of the Patton porphyry intrusion, ~1432 m asl) and Mount Cockfield (1856 m asl) 20 km to the southeast (Fig. 2).

Bedrock geology

The Casino deposit area is underlain by metamorphosed and deformed basement rocks of the Yukon-Tanana terrane, an allochthonous tectonic terrane that extends over 2000 km from Alaska, through Yukon and south into British Columbia (Allan et al., 2013; Mortensen and Friend, 2020). The terrane consists of rocks formed in a Mid- to Late Paleozoic continental arc system that separated the Yukon-Tanana arc from the western margin of Laurentia (Nelson et al., 2006; 2013). The terrane consists of the Snowcap assemblage of metamorphosed sedimentary and minor volcanic rocks which is unconformably overlain by the Finlayson, Klinkit and Klondike assemblages, predominantly arc metavolcanic and associated metasedimentary rocks (Fig. 2) (Ryan et al., 2013; Colpron et al., 2006; 2016).

The bedrock geology of the deposit and surrounding area is briefly summarized below from (Archer and Main, 1971; Godwin, 1975; 1976; Bower et al., 1995; Ryan et al., 2013; Casselman and Brown, 2017; Yukon Geological Survey 2020k; 2020m). The Casino deposit is classified as a calc-alkaline porphyry deposit and is centered on the Patton Porphyry, a Late Cretaceous (72-74 Ma) stock that intrudes the Mesozoic Dawson Range Batholith and Paleozoic Yukon Crystalline Complex schists and gneisses. The intrusion of the small porphyry into these older rocks caused brecciation along its contacts. The porphyry is locally mineralized and is surrounded by a potassically-altered intrusion breccia at its outer contacts. Elsewhere, the porphyry consists of discontinuous dikes (up

to 10s of m wide) that cut both the porphyry and Dawson Range Batholith. The overall composition of the porphyry is rhyodacite, with phenocrysts of dacite composition and a matrix of quartz latite composition.

Primary copper, gold and molybdenum mineralization was deposited from hydrothermal fluids in the contact breccias and fractured wall rocks and consists of pyrite, chalcopyrite, molybdenite, and minor huebnerite. Supergene mineralization is concentrated within the mineral assemblages corresponding to both the phyllic zone and surrounding weakly developed argillic and propylitic zones. Grades decrease away from the contact zone towards the centre of the stock and outward into the wall rocks.

Godwin (1975; 1976) suggested that the warm and wet climate of the Paleogene (Zachos et al., 2001; Moran et al., 2006; Vavrek et al., 2012) was the likely time frame for supergene enrichment of the deposit. During this period, the deposit was subjected to deep (up to 300 m) chemical weathering because of the porous nature of the breccias and strongly altered zones. The deep weathering profile is largely intact because of minimal to no glacial erosion of the region during the last 2 million years (Bond et al., 2010; Bond and Lipovsky, 2012). Thus, the deposit exhibits a well-formed zonation consisting of a leached cap, supergene oxide mineralization, supergene sulfide mineralization, and hypogene (primary) mineralization. The leached cap is on average 70 m thick, enriched in gold, depleted in Cu, and consists primarily of boxwork textures filled with jarosite, limonite, goethite, and hematite. The deep weathering has obliterated bedrock textures and replaces most minerals with clay. The supergene oxide zone consists of a few isolated lenses within the leached cap and is thought to have formed by more recent fluctuations in the water table. It is Cu-rich and contains chalcanthite, malachite, brocanthite along with minor cuprite, azurite, tenorite, neotocite, and trace molybdenite as coatings on fractures and in vugs. The supergene sulfide zone underlies the leached cap, is on average 60 m thick and outcrops at surface in places. The supergene zone Cu grades commonly almost double those in the hypogene zone and contains pyrite, chalcopyrite, bornite, and tetrahedrite that may be altered along grain boundaries to chalcocite, digenite, or covellite, as well as molybdenite that is locally altered to ferrimolybdite. Hypogene mineralization underlies the supergene sulfide zone and consists of pyrite, chalcopyrite, molybdenite, sphalerite, bornite, and tetrahedrite. In the hypogene zone, gold occurs as discrete grains (50-70 µm) in quartz and as inclusions in pyrite and chalcopyrite (1-15 µm). On the eastern and northern flanks of the deposit, the supergene oxide zone is absent, the other zones are thinner, and the hypogene zone is closest to surface (<25 m).

Mineral occurrences near the Casino deposit are shown on Figure 2 and listed in Table 1. They include porphyry Cu-Mo-Au occurrences on Mount Cockfield 20 km to the southeast (Yukon Geological Survey, 2020c) and west of the Casino deposit (Zappa, Canadian

Creek; Yukon geological Survey 2020g, j). Additional polymetallic vein occurrences are located 10 km northeast of Casino (Marquerite; Yukon Geological Survey, 2020b), 10 km east (Nordex, Idaho; Yukon Geological Survey, 2020d, i) and 12 km southeast (Rude Creek; Yukon Geological Survey, 2020l). Two gold occurrences have been reported 13 to 16 km east-northeast of the deposit (Buck and Mascot; Yukon Geological Survey, 2020a, h).

Table 1. Summary of known mineral occurrences in the study area. Data from Yukon Geological Survey (2020e, c, g, j, b, i, l, a, h, d).

Name	Occurrence Number	Type	Reference
Bomber	115J 027	Vein Polymetallic Ag-Pb-Zn+/-Au	YGS, 2019a
Cockfield	115J 017	porphyry Cu-Mo-Au	YGS, 2019e
Zappa	115J 036	porphyry Cu-Mo-Au	YGS, 2019f
Canadian Creek	115J 101	porphyry Cu-Mo-Au	YGS, 2019g
Marquerite	115J 070	Porphyry-related Au, Vein Polymetallic Ag-Pb-Zn+/-Au	YGS, 2019h
Nordex	115J 023	Vein Polymetallic Ag-Pb-Zn+/-Au	YGS, 2019i
Idaho	115J 099	Porphyry-related Au, Vein Polymetallic Ag-Pb-Zn+/-Au	YGS, 2019j
Rude Creek	115J 022	Vein Polymetallic Ag-Pb-Zn+/-Au	YGS, 2019k
Buck	115J 071	orogenic Au, plutonic related Au	YGS, 2019l
Mascot	115J 074	orogenic Au, Au-Ag-As	YGS, 2019m

Surficial geology

The surficial geology of the Casino area is summarized below from maps and reports published previously (Duk-Rodkin, 2001; 2002; Huscroft, 2002a, c, b; Duk-Rodkin et al., 2004; Bond and Sanborn, 2006; Bond et al., 2010; Bond and Lipovsky, 2012; Lipovsky and Bond, 2012; McKillop et al., 2013). The local landscape is largely unglaciated and as a result, bedrock in the region is weathered and leached. Bedrock outcrop and tors (rocky peaks) are common along the ridges and summits and have disintegrated *in situ* by mechanical (freeze/thaw) and/or chemical weathering. Surficial material in upland areas flanking ridges and tors consists of colluvium and weathered bedrock intermixed with variable amounts of loess. Material moves downslope by gravity-driven processes such as creep, solifluction, landslides, and snow avalanches, and it is these processes that feed debris that eventually ends up in creeks. Lower lying areas are covered with loess.

Isolated alpine glaciers existed on Mount Cockfield that extended west into the headwaters of Victor and Colorado creeks tributary valley and eastward into an unnamed tributary that drains into the Selwyn River during the Reid glaciation (middle Pleistocene) (Bond and Lipovsky, 2012). Glacial sediments (end moraines) and cirques are present on the east flank of Mount Cockfield. Stream sediments in the creeks draining this east flank are, in part, derived from the glacial deposits. Evidence of past glaciation also exists in the headwaters of Canadian Creek, immediately northwest of Patton Hill, where cirques were formed

during early Pleistocene (preReid) glaciation (Duk-Rodkin, 2001; Duk-Rodkin, 2002; 2004; Bond and Lipovsky, 2012) (Fig. 5).

The study area is a periglacial environment; the land surface is subject to seasonal freeze-thaw cycles and cryoturbation. Permafrost is widespread but discontinuous and is most common on north-facing slopes and in the bottoms of valleys that are covered by thick colluvium and organic veneers. Presence of permafrost is indicated by solifluction lobes, pingos, and thermokarst features. Frost shattering, cryoturbation, solifuction soil creep, and land sliding are all mechanisms by which bedrock is released into the surficial environment and unconsolidated sediments move down slope and into creeks Bond and Lipovsky (2012). Fluvial erosion of older gravel deposits, including placers, also contribute material to modern creeks.

First and second order streams (e.g., Casino Creek) are found in narrow V-shaped valleys and contain subangular to subrounded gravel to boulders that are derived from local bedrock. Higher order streams occur in broader valleys and are filled with more distally derived colluvium, loess, and rounded gravel (e.g., Dip Creek, Colorado Creek). Bond and Lipovsky (2012) reported that understanding the relationship between valley morphology and the variable texture and sources of fluvial sediments is important for sampling and interpreting stream silt geochemical surveys. Because loess content in fluvial sediments is variable, they recommended that stream samples ideally should be collected from high-energy streams in narrow valleys where the loess content is lowest.

METHODS

Field Methods

A total of 24 stream water samples were collected from 22 sites downstream of the deposit (Fig. 2) and in background areas by the GSC in September 2017 using GSC National Geochemical Reconnaissance (NGR) sampling protocols similar to those previously reported (Day et al., 2013; McCurdy and McNeil, 2014). Field duplicate samples were collected at two sites: 115J17-1005 is a duplicate of sample 115J17-1004 and 115J17-1024 is a field duplicate of 115J17-1023. Appendix A1 lists sample location and site data. Field blanks were filtered and preserved using the same methods as for sampling site groundwater. Colour photographs of each water sample site are presented elsewhere (McCurdy et al., 2019).

Two water samples were collected in the mid-channel of streams at each site: i) a filtered sample, acidified on arrival at the laboratory (‘FA’) for major and trace elements; and ii) a filtered, un-acidified sample (‘FU’) for anions, alkalinity, and DOC. On-site, 60 ml of water was collected by filling the syringe from the active part of the stream channel and filtered through a single-use Millipore Sterivex-HV® 0.45 μm filter unit attached to a 60

ml sterile plastic syringe into each of the triple rinsed FA and FU 60 ml Nalgene® bottles. In-situ water measurements were completed using a YSI Pro Plus® multi-parameter meter. The instrument simultaneously measured temperature, pH, conductivity, dissolved oxygen (DO), oxidation-reduction potential (ORP) with automatic temperature compensation for pH and dissolved oxygen. Field instrumentation was calibrated daily before fieldwork. Accuracy and units of measurement for each parameter are listed in Table 2.

Table 2. Summary of variables determined in water samples using the YSI Pro Plus® multi-parameter meter.

	Range	Accuracy	Resolution	Units of measurement
Dissolved Oxygen (%)	0-500%	0 to 200% (±2% of reading or 2% air saturation, whichever is greater)	1% or 0.1% air saturation	%
Temperature	-5 to 70°C	±0.2°C	0.1°C	°C
Conductivity	0 to 200 mS/cm	±0.5% of reading or 0.001 mS/cm, whichever is greater	0 to 500 µS/cm=0.001; 501 to 5000 µS/cm=0.01	µS
pH	0 to 14 units	±0.2 units	0.01 units	pH units
Oxidation-Reduction Potential (ORP)	-1999 to +1999 mV	±20 mV in redox standards	0.1 mV	mV
Air Pressure	375 to 825 mmHg	±1.5 mm Hg from 0 to 50°C	0.1 mmHg	kPa

Nine groundwater samples from eight locations (Fig. 2) were collected from monitoring wells during the same period by Western Copper and Gold Corporation. Sample water was collected using a low flow (0.2 to 0.5 L/min) submersible pump positioned 1 m above the screen height in the well (Knight Piésold Ltd , 2015). Field parameters for well waters were measured from groundwaters pumped to the surface and measured using a flow-thru cell attached to a calibrated multi-parameter probe (Knight Piésold Ltd, 2015). One sample was a blank (L1992155-2) that consisted of distilled/deionized water provided by the analytical laboratory. The distilled/deionized water was added to the sample bottle using the same field techniques as the other samples, including field filtration and field preservation. Field and travel blanks were inserted into the sample suite using the same methods and parameters as the sample suite. Sample L1992155-10 is a field duplicate of sample L1992155-9. Samples for total metals were collected in 120 mL acid-washed plastic bottles and preserved in the field with laboratory-supplied ultrapure nitric acid. Samples for dissolved metals were filtered in the field through 0.45 µm disposable filters and preserved with laboratory-supplied ultrapure nitric acid immediately after filtration. These samples

were shared with the GSC after splits were analyzed by Western Copper and Gold Corporation.

Laboratory Methods

The filtered stream water samples collected by GSC were kept cool and in the dark until being received at the GSC's Inorganic Geochemistry Research Laboratory, Ottawa, where they were acidified within 48 hours of arrival with 0.5 mL 8M Ultrapure HNO_3 and left at room temperature for a period of 1 month. The unacidified samples were stored in a fridge at 6^{o}C. A filtered unacidified aliquot is transferred for each samples to a polypropylene test tube just prior to analysis for pH, Conductivity, Anions, Alkalinity and DOC. Groundwaters collected from monitoring wells were submitted for analysis to ALS Environmental (Burnaby). Details of ALS laboratory methods are included in Knight Piésold Ltd. (2015).

Conductivity and pH of stream waters

Conductivity and pH measurements at GSC were made using an Accumet AR50 dual channel pH/ion/conductivity meter with temperature compensation. The pH measurements were made using a Thermo Fisher Accumet combination double junction Ag/AgCl electrode (PN 13-620-221) and calibrated using pH 4.00, 7.00, and 10.00 buffers. The conductivity measurements were made using Thermo Fisher Accumet 4-cell conductivity probes with automatic temperature compensation, with a 1.0 cm^{-1} cell constant (PN 13-620-165) for samples in the 10 to 2000 µS cm^{-1} range and a 10.0 cm^{-1} cell constant (13-620-166) for samples in the 1000 to 200,000 range. Commercial conductivity standards were used for calibration. Data are listed in Appendix B1, worksheet 4 entitled 'ALK COND PH'.

Alkalinity of stream waters

Alkalinity measurements at GSC were completed using a Mantech PC-Titrate^{TM} system with a Titra-Sip^{TM} Module on the FU samples. Total alkalinity was measured by potentiometric titration with 0.02 N H_2SO_4. Software determined the volume of acid required to reach the bicarbonate equivalence point. Alkalinity results are reported as equivalents of $CaCO_3$ in ppm. Data are listed in Appendix B1, worksheet 4 entitled 'ALK COND PH'.

Dissolved Organic Carbon of stream waters

Total Organic Carbon (TOC) analysis was completed at GSC with a Shimadzu TOC-L analyser using a 680 °C combustion catalytic oxidation method combined with NDIR detection. This was reported as Dissolved Organic Carbon (DOC) on a 0.45 µm Durapore®-filtered (FU) sample. In environmental and water samples where the inorganic carbon (IC) concentration may be high, the (total or dissolved) organic carbon is measured by a non-purgeable organic carbon (NPOC) method. This method is the same as the TOC

combustion measurement method with the addition of acidification and sparging to remove the inorganic carbon (IC) in the sample prior to TOC analysis. Data are listed in Appendix B1, worksheet 5 entitled 'DOC'.

Anions of stream waters

Anion analysis was completed at GSC using a Dionex ICS 2100 Ion Chromatograph fitted with an AS-AP auto-sampler. Bromide, chloride, fluoride, nitrate, phosphate, and sulfate were separated by Ion Chromatography using a three-step gradient elution (12 to 52 mmol KOH eluant) with an AS-18 column. The anion concentrations were quantified using conductivity in comparison with known concentration calibration standards and Dionex Chromeleon software. Table 2 lists the anions reported with the corresponding lower detection limit. Data are listed in Appendix B1, worksheet 3 entitled 'ANIONS'.

Trace and Major Element analysis of stream waters

Acidified and filtered stream water samples were analyzed for trace metal and major elements at GSC Laboratories in Ottawa. A complete list of elements and detection limits are given in Table 3. Trace metal analysis was performed using a Thermo X Series II quadrupole inductively coupled plasma mass spectrometer (ICP-MS) with Xt cones, PlasmaScreen fitted, standard concentric nebulizer and Peltier cooled conical impact bead spray chamber (3 °C) using Rh and Ir as internal standards. Most elements measured and corrections for spectral interferences are detailed in Hall et al. (1995; 1996). Data for Hf and Zr are not published because these elements are not sufficiently stabilized in water by the addition of nitric acid. Data for In, Se, Ag, Ta, and Tl are not published because of inadequate detection limits and/or precision. Data are listed in Appendix B1, worksheet 2 entitled 'ICPMS'.

Table 3. Anions determined by Ion Chromatography for filtered-unacidified (FU) surface water samples.

Anions	Lower Detection	Units of Measure
Br	0.02	mg/L
Cl	0.01	mg/L
F	0.01	mg/L
NO_3	0.02	mg/L
PO_4	0.02	mg/L
SO_4	0.02	mg/L

Major element analysis was performed using an axial Spectro Arcos Inductively Coupled Plasma Optical Emission Spectrometer (ICP-OES) using a 1 % $CsNO_3$ buffer (1:5 ratio) as a matrix modifier with a Burgener Teflon Mira Mist Nebulizer (uptake rate 1 mL/min) and a cyclonic spray chamber. The argon flowrates are coolant 14.5 L/min^{-1}, auxiliary 0.9

L/min^{-1}, and nebulizer 0.8 L/min^{-1}. The RF power was set at 1500 watts. Inter-element correction factors were applied as required to correct for various spectral interferences. Data for Sc are not published because of inadequate detection limits and/or precision. Data are listed in Appendix B1, worksheet 1 labelled 'ICPES'. The calculated charge errors for the ground and surface waters are all significantly less than 5% for all samples.

Isotopic analyses of stream and ground waters

Water samples were analyzed for $\delta^{18}O$, $\delta^{2}H$, and $\delta^{34}S_{SO4}$ (for samples with sufficient SO_4^{2-}) and $^{87}Sr/^{86}Sr$ at Queen's Facility for Isotope Research (QFIR). Data are listed in Appendix B2. For $\delta^{18}O$, samples were analyzed via CO_2 equilibration. Approximately 2 mL samples were loaded into 10 mL exetainer vials, purged with a mixture of 3 % CO_2 in He and allowed to equilibrate for 3 days. The equilibrated CO_2 was analyzed using a Thermo-Finnigan Gas Bench coupled to a Thermo-Finnigan DeltaPlus XP Continuous-Flow Isotope-Ratio Mass Spectrometer (CF-IRMS). The $\delta^{18}O$ values are reported using the delta (δ) notation in permil (‰), relative to Vienna Standard Mean Ocean Water (VSMOW), with a precision of 0.2 ‰. For $\delta^{2}H$, samples were analyzed via thermo-chemical reduction. Samples were loaded into 1 mL vials and introduced into a Thermo-Finnigan H-Device via an airtight syringe, flash evaporated and reduced by contact with a chromium reaction furnace at 850 °C. The hydrogen isotopic composition of the H_2 gas is measured via the dual inlet system of a Thermo-Finnigan MAT 253 IRMS. The $\delta^{2}H$ values are reported using delta (δ) notation in permil (‰), relative to VSMOW, with a precision of 1 ‰.

For $\delta^{34}S$ of dissolved sulfate, samples were precipitated as $BaSO_4$ by adding excess $BaCl_2$ to aliquots of acidified waters; the precipitate was then weighed into tin capsules and the sulfur isotopic composition was measured using a MAT 253 IRMS coupled to a Costech ECS 4010 Elemental Analyzer. The $\delta^{34}S$ values are calculated by normalizing the $^{34}S/^{32}S$ values in the sample to that in the Vienna Canyon Diablo Troilite (VCDT) international standard. Values are reported using the delta (δ) notation in units of permil (‰) and are reproducible to 0.2 ‰.

Strontium isotope separation was achieved using a method adapted from Smet et al. (2010), utilizing a prepFAST-MC™ automated column chromatography system (Romaniello et al., 2015). Strontium-specific exchange resin Sr Spec™ was loaded into a Poly-Prep column (3 cm x 200 µL) and pre-washed with 4 mL of 8 N HNO_3 and 1 mL of 3 N HNO_3, at a flow rate of 500 µL/min. Dried samples were dissolved in 3 N HNO_3 and a 1 mL sample aliquot loaded onto the column at a flow-rate of 250 µL/min. Matrix elements were eluted using 3 mL of 3 N HNO_3 and a purified Sr aliquot was eluted using 1 mL of 0.05 N HNO_3, both at a flow rate of 500 µL/min. Procedure blanks, along with certified reference materials; NASS-7 (NRC, 2016), and SLRS-5 (NRC, 2015) were included in each batch.

Isotopic measurements were conducted using a ThermoFinnigan Neptune™ Series High Resolution Multicollector ICP-MS (MC-ICPMS) coupled with an Elemental Scientific Inc (ESI, Nebraska) Microfast autosampler at QFIR. Prior to analysis all samples were refluxed with 200 µL of 15.8 N HNO_3 at 180 °C, evaporated at 80 °C and dissolved into 2 % HNO_3. Sample was delivered at 30 µL/minute using a PFA nebulizer and a cyclonic double-pass spray chamber composed of quartz. External measurement precision was monitored using NIST-SRM-987 isotopic standard and mass bias correction achieved using $^{86}Sr/^{88}Sr$ values ($^{86}Sr/^{88}Sr = 0.1194$).

RESULTS

Major ions and field parameters

Ground and surface water pH values range from 5.4 to 8.3 (Appendix C, Map 2); values that are typical for ground and surface waters in crystalline rock systems (Leybourne et al., 2006). Ground and surface waters from the Casino study area are dominantly Ca-HCO_3 to Ca-SO_4-type waters (Fig. 4).

Major and trace element data in for the ground and stream water samples is included in Table 4. Groundwater samples typically have higher salinities, with total dissolved solids (TDS) ranging from 74 to 1320 mg/L, whereas surface waters range from 98 to 654 mg/L (Figs. 4 and 5). Groundwater salinities are also higher proximal to the Casino deposit (Fig. 4), whereas surface water salinities are highest in streams draining to the north of the deposit (see Appendix C, Map 3). Surface and groundwaters are dominated by Ca (and Mg) as the major cations, with only four samples showing slightly elevated Na concentrations (14-20 mg/L; Fig. 5) and only three water samples trending to the Na (+K) apex of the piper plot (Fig. 4). All waters have low Cl (< 1 mg/L) and F (< 1 µg/L) concentrations. Anions are dominated by HCO_3 and, for groundwaters close to the Casino deposit, SO_4^{2-} (groundwaters are up to 800 mg/L SO_4^{2-}).

Table 4. Major and trace elements determined by ICP-MS/ES for filtered-acidified (FA) and unfiltered-acidified (UA) water samples

Element	Limit Detection Limit	Units of Measure	Analytical Method	Element	Limit Detection Limit	Units of Measure	Analytical Method
Ag	0.005	µg/L	ICP-MS	Mo	0.05	µg/L	ICP-MS
Al	2	µg/L	ICP-MS	Na	0.05	mg/L	ICP-ES
As	0.1	µg/L	ICP-MS	Nb	0.01	µg/L	ICP-MS
B	0.5	µg/L	ICP-MS	Nd	0.005	µg/L	ICP-MS
Ba	0.2	µg/L	ICP-MS	Ni	0.2	µg/L	ICP-MS
Be	0.005	µg/L	ICP-MS	P	0.05	mg/L	ICP-ES
Bi	0.02	µg/L	ICP-MS	Pb	0.01	mg/L	ICP-ES
Br	0.05	mg/L	ICP-ES	Pr	0.005	mg/L	ICP-ES
Ca	0.02	mg/L	ICP-ES	Rb	0.05	µg/L	ICP-MS
Cd	0.02	µg/L	ICP-MS	Re	0.005	µg/L	ICP-MS
Ce	0.01	µg/L	ICP-MS	S	0.05	mg/L	ICP-ES
Cl	0.1	mg/L	ICP-ES	Sb	0.01	µg/L	ICP-MS
Co	0.05	µg/L	ICP-MS	Sc	0.001	mg/L	ICP-ES
Cr	0.1	µg/L	ICP-MS	Se	1	mg/L	ICP-ES
Cs	0.01	µg/L	ICP-MS	Si	0.02	mg/L	ICP-ES
Cu	0.1	µg/L	ICP-MS	Sm	0.005	µg/L	ICP-MS
Dy	0.005	µg/L	ICP-MS	Sn	0.01	µg/L	ICP-MS
Er	0.005	µg/L	ICP-MS	Sr	0.5	µg/L	ICP-MS
Eu	0.005	µg/L	ICP-MS	Ta	0.01	µg/L	ICP-MS
Fe	0.005	mg/L	ICP-ES	Tb	0.005	mg/L	ICP-ES
Ga	0.01	µg/L	ICP-MS	Te	0.02	µg/L	ICP-MS
Gd	0.005	µg/L	ICP-MS	Ti	0.5	µg/L	ICP-MS
Ge	0.02	µg/L	ICP-MS	Th	0.02	µg/L	ICP-MS
Hf	0.01	µg/L	ICP-MS	Tl	0.005	µg/L	ICP-MS
Ho	0.005	µg/L	ICP-MS	Tm	0.005	µg/L	ICP-MS
In	0.01	µg/L	ICP-MS	U	0.005	µg/L	ICP-MS
K	0.05	mg/L	ICP-ES	V	0.1	mg/L	ICP-ES
La	0.01	µg/L	ICP-MS	W	0.02	µg/L	ICP-MS
Li	0.02	µg/L	ICP-MS	Y	0.01	µg/L	ICP-MS
Lu	0.005	µg/L	ICP-MS	Yb	0.005	µg/L	ICP-MS
Mg	0.005	mg/L	ICP-ES	Zn	0.5	mg/L	ICP-ES
Mn	0.1	µg/L	ICP-MS	Zr	0.5	mg/L	ICP-ES

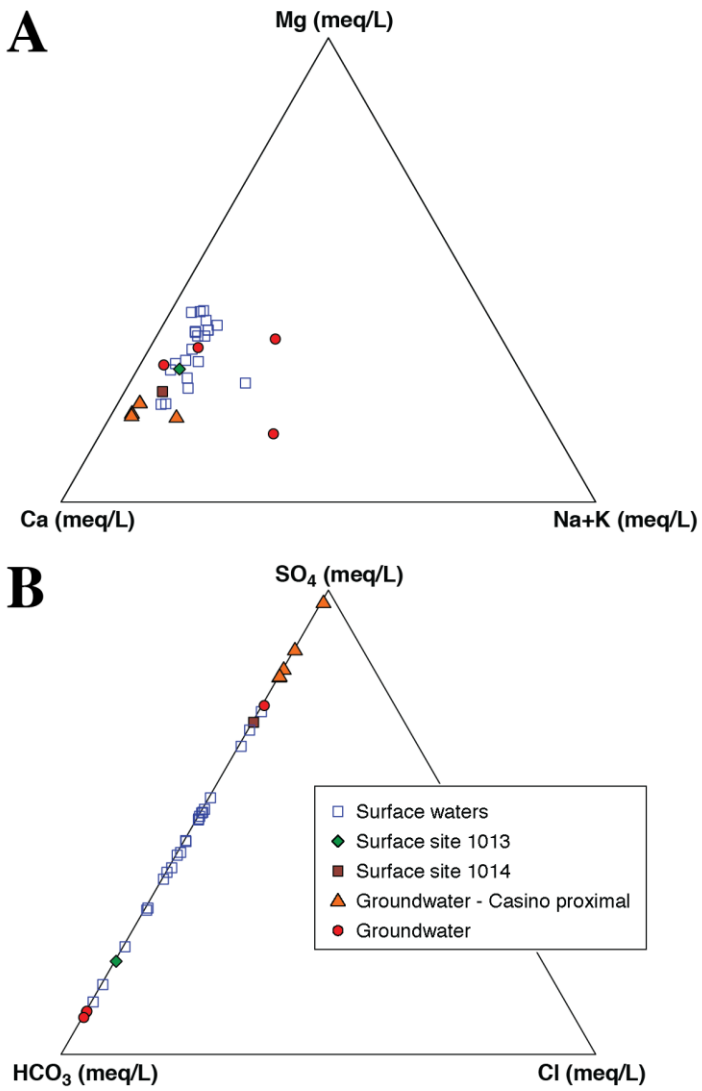

Figure 4. Modified Piper plot of ground and surface waters from the Casino deposit area. A) cations, and B) anions. Waters closest to the Casino deposit have proportionally higher SO_4^{2-} and Ca concentrations and the highest TDS.

Trace elements

Several trace elements were found to be below detection, including Ag, Bi, Ga, Ge, In, Hf, Nb, P, Sc, Sn, Ta, Tl, and W. We have plotted some of the trace elements in ground and surface waters with respect to dissolved SO_4^{2-} concentrations (Fig. 6) rather than TDS, because oxidation of sulfide minerals is a primary mechanism for increasing SO_4^{2-} in shallow waters in crystalline terrains; there are no chemical (evaporite) sediments in the catchment (Fig. 2), consistent with the sulfur isotope values (discussed below). Therefore, correlations between trace elements and SO_4^{2-} could be indicative of solutes released from sulfide oxidation in the waters.

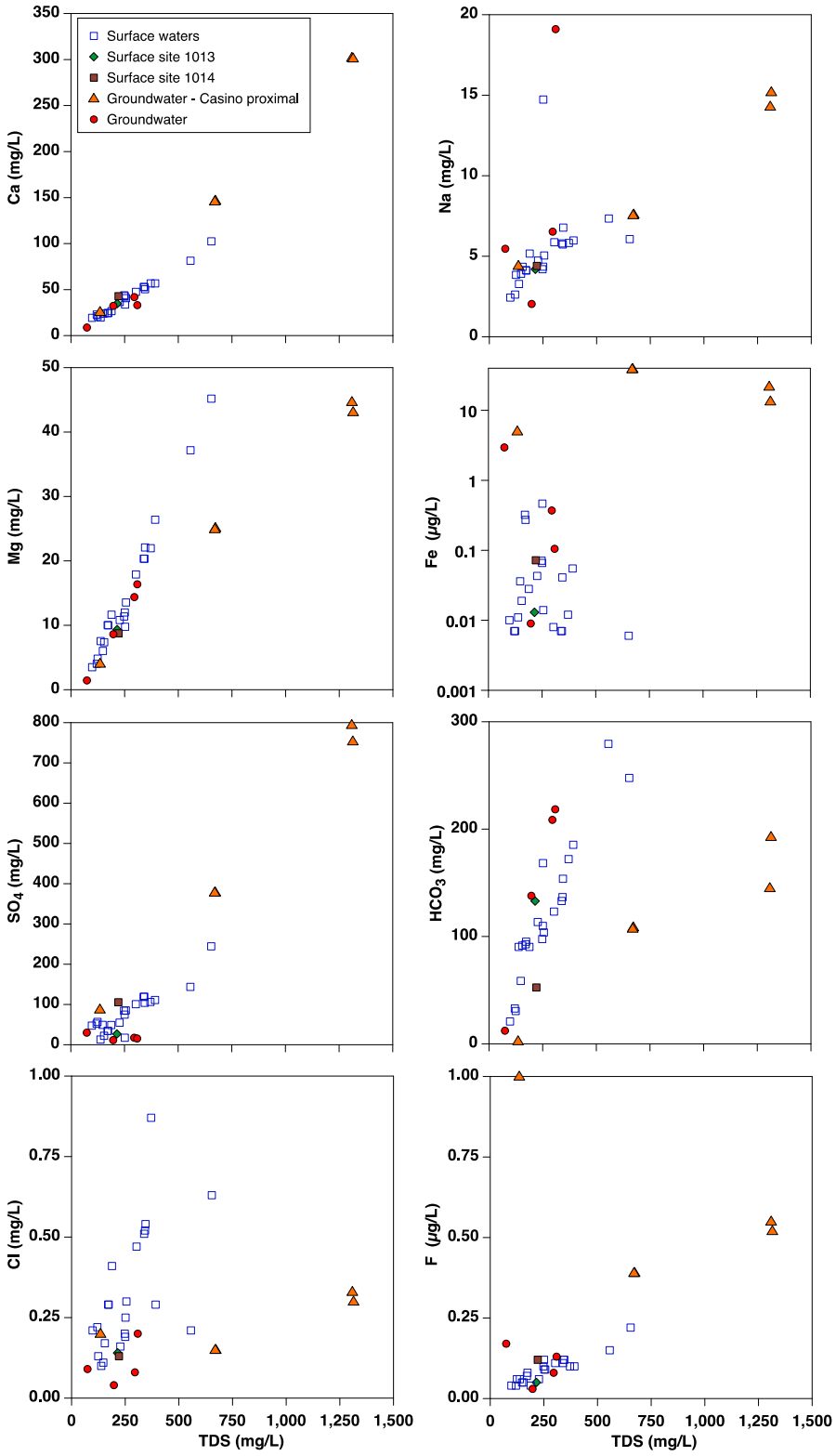

Figure 5. Plots of major ions and Fe, F versus total dissolved solids (TDS) for Casino surface and groundwaters

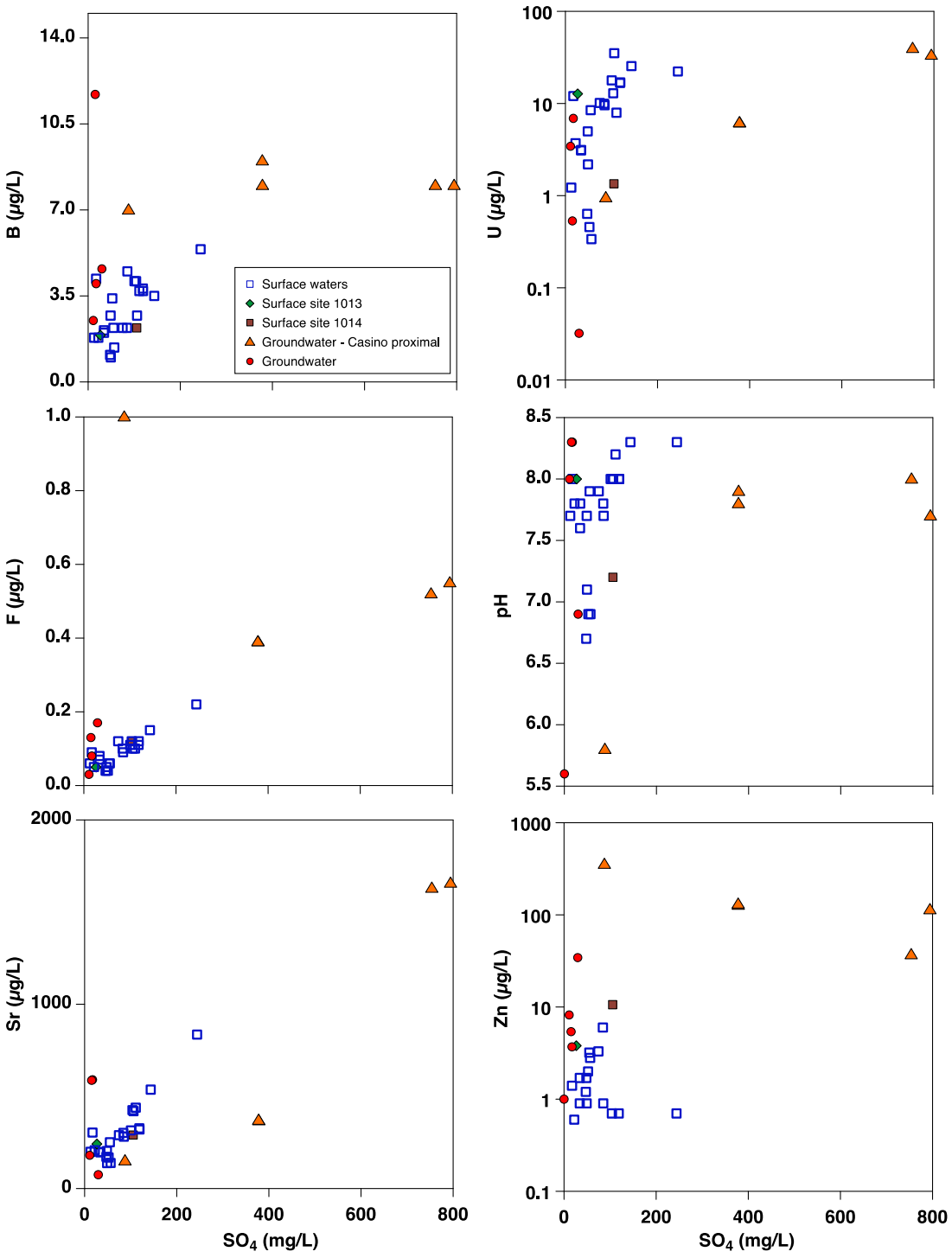

Figure 6A. Plots of trace elements (B, U, F, Sr, and Zn) and pH versus SO_4^{2-} concentrations for Casino surface and groundwaters.

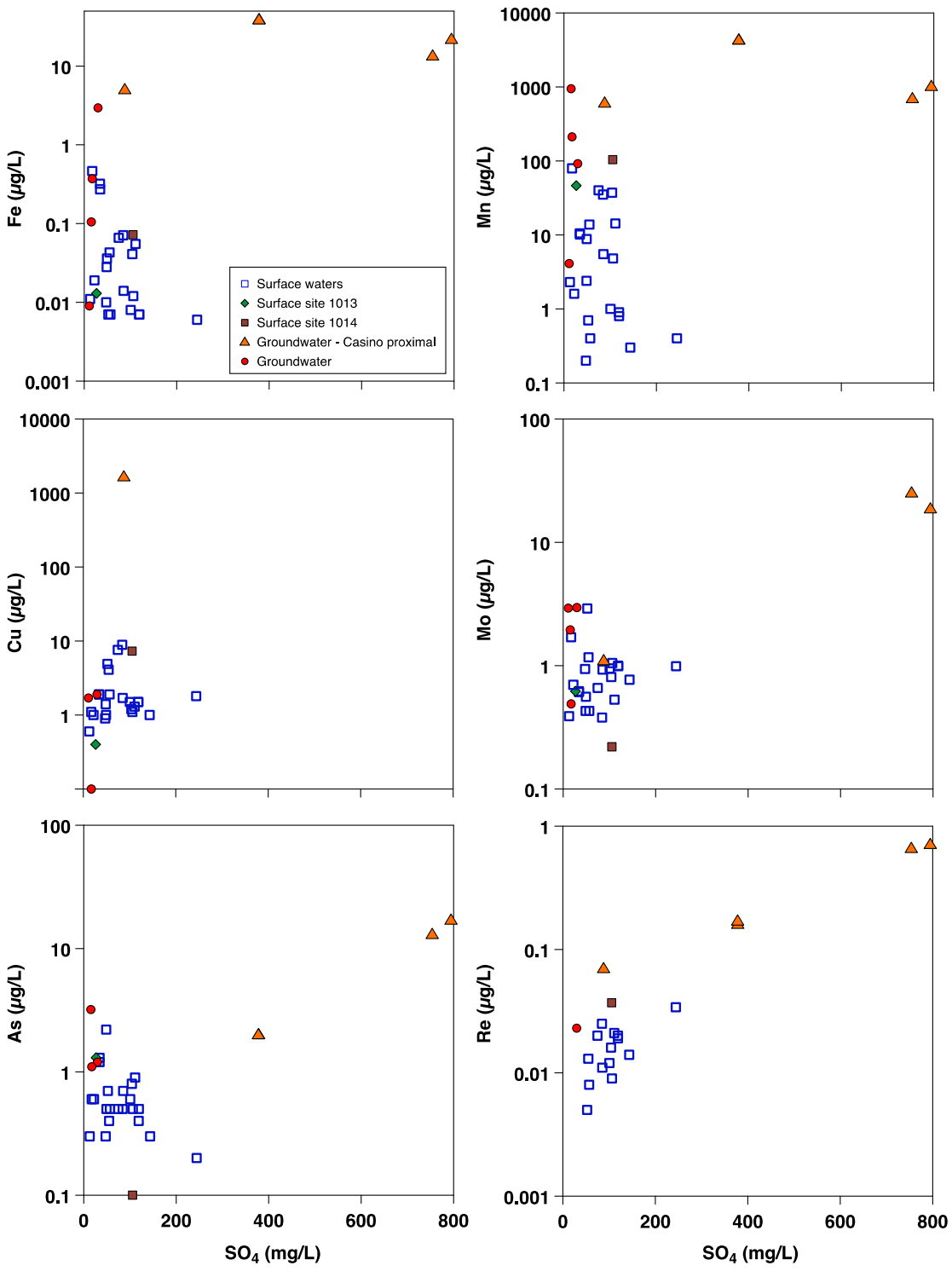

Figure 6B. Plots of trace elements (Fe, Mn, Cu, Mo, As, and Re) versus SO_4^{2-} concentrations for Casino surface and groundwaters.

Iron concentrations for most waters are generally low (<0.1 mg/L), typical of surface waters exposed to atmospheric O_2. By contrast, the more saline, higher sulfate groundwaters have elevated Fe and Mn concentrations (<40 mg/L and 5,000 µg/L, respectively). Dissolved Fe and Mn concentrations correlate with the physicochemical conditions of the waters, with the highest concentrations correlating with the reduced groundwater conditions (<0 mV). Groundwaters with elevated Fe and Mn also have elevated Cu, Mo, As, Re, B, U, and Zn concentrations, with values up to >1500, 25.2, 17, 0.71, 11.7, 39.6, and 354 µg/L, respectively. Generally, samples with highest sulfate concentrations have the highest metal and metalloid concentrations.

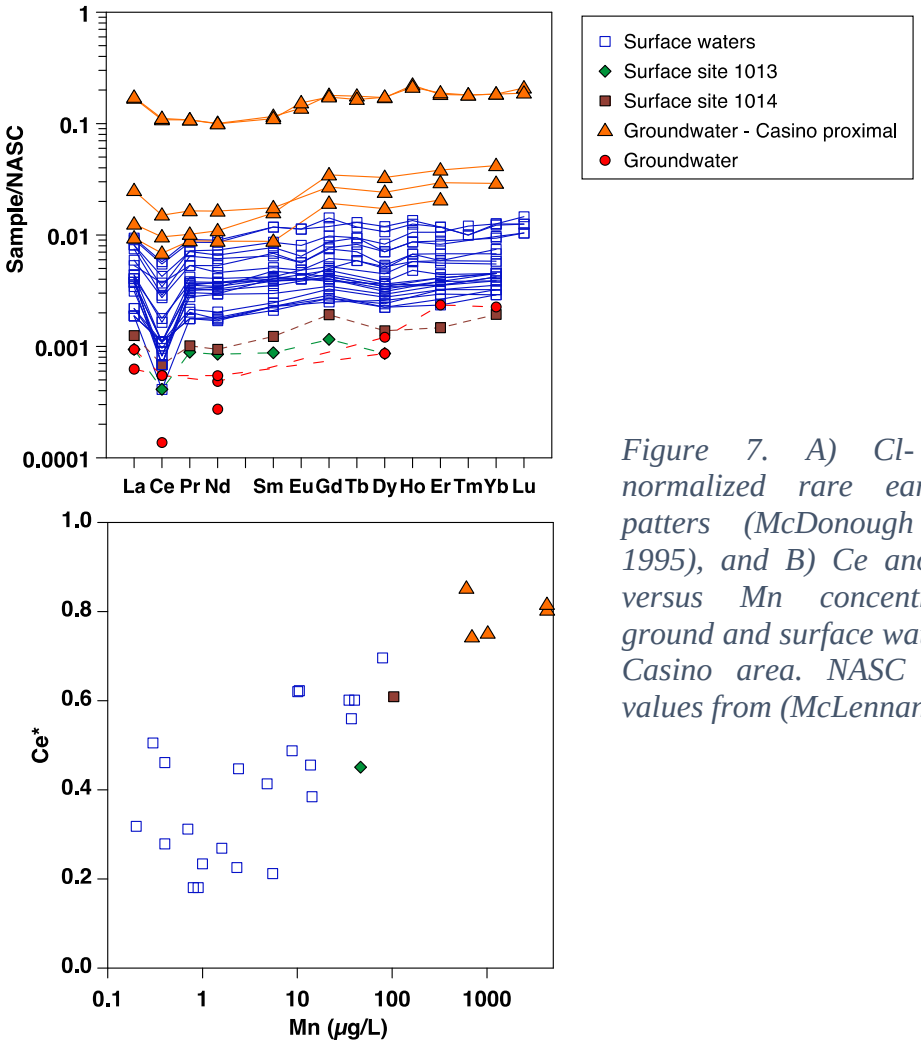

Figure 7. A) Cl- chondrite-normalized rare earth element patters (McDonough and Sun, 1995), and B) Ce anomaly (Ce) versus Mn concentrations for ground and surface waters from the Casino area. NASC normalizing values from (McLennan, 1989).*

Rare earth elements

Rare earth element (REE) concentrations were above detection limit for most of the waters. General REE profiles allow for the evaluation of the interconnectivity of ground and surface waters (Fig. 7A). All waters have relative flat to slightly light REE-enriched profiles normalized to North American Shale Composite (NASC; Gromet et al., 1984), but

slightly LREE enriched normalized to chondrite (McDonough and Sun, 1995). Groundwaters proximal to the Casino deposit have higher total REE concentrations compared to the surface waters (up to 22 µg/L versus up to 1.5 µg/L). All samples show subtle to significant Ce anomalies (where Ce* = [Ce]NASC/([La]NASC* [Gd]NASC)^0.5), with Ce* ranging from 0.18 – 0.82. There is a positive correlation (r = 0.841; p < 0.0001 for Ce* vs Log10[Mn]) between the Ce* value and Mn concentrations in the waters; groundwaters are more reducing with higher Mn and less pronounced Ce* anomaly than surface waters (Fig. 7B).

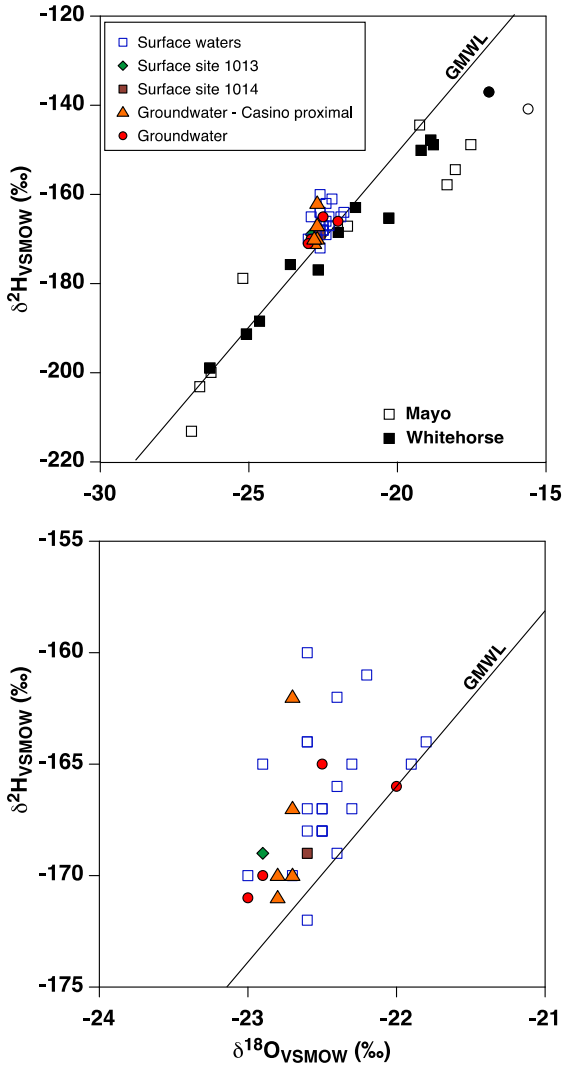

Figure 8. Oxygen and hydrogen isotopic composition of Casino surface and groundwaters, including the Global Meteoric Water Line (GMWL) (Craig, 1961). A) Also included are monthly weighted averages for precipitation at monitoring stations at Mayo and Whitehorse, Yukon. Data from IAEA/WMO (2019). Global Network of Isotopes in Precipitation. The GNIP Database. Accessible at: https://nucleus.iaea.org/wiser. B) Expanded view of Casino waters and the GMWL.

Stable isotopic composition of water and dissolved sulfate

The Isotopic fractionations of $\delta^{18}O$ and $\delta^{2}H$ produces recognisable trends which relate to distinct geochemical processes, such as evaporation, mixing, recharge, and source. These trends are discernible by plotting $\delta^{18}O$ versus $\delta^{2}H$ (Fig. 8A and B). Surface water samples

range from -23.0 to -21.8 ‰ and -172 to -160 ‰, respectively. The data are tightly clustered around the mean annual weighted average for precipitation in the Yukon, as recorded at stations in Mayo and Whitehorse (Fig. 8A). Groundwaters are isotopically indistinguishable from the surface waters; all data plot on or slightly above the global meteoric water line, with excess "d" values of 13.5 ± 2.84 ‰ (range = 9.2 to 21.1 ‰) (Fig. 8B).

There was sufficient SO_4^{2-} to measure the S isotopes in 16 of the surface water samples, with resulting $\delta^{34}S$ values ranging from 3.9 to 14.1 ‰ (Fig. 9A). Dissolved sulfate in Casino surface waters plots well below different sources of terrestrial or marine sulfate. Seven groundwater samples have variable $\delta^{34}S$ values, ranging from -0.3 to 7.4 ‰, with lowest values in groundwaters proximal to mineralization and having the highest SO_4^{2-} concentrations (Fig. 9A).

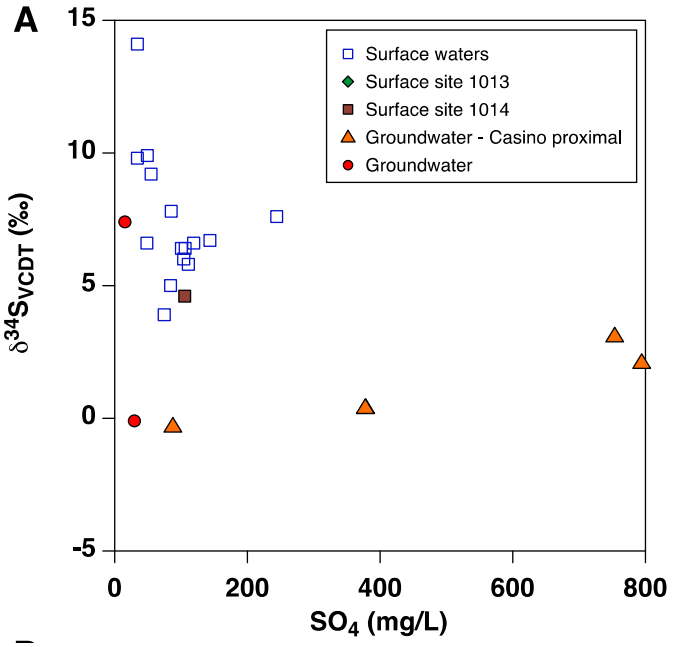

Figure 9. $\delta^{34}S$ versus SO_4^{2-} concentrations for dissolved sulfate in Casino surface and groundwaters.

Isotopic composition of Sr

Nineteen waters were analyzed for their Sr isotopic composition. Strontium isotopes are useful in hydrogeochemical studies because surface processes such as evaporation, precipitation or adsorption do not fractionate strontium isotopes (McArthur, 1994). They can be used to differentiate solute sources, be it rainfall, water-rock interaction, or wind-dispersed materials such as dust, and identify fluid pathways and mixing zones. Comparing $^{87}Sr/^{86}Sr$ composition to the Sr/Rb and conservative elements Na/Cl allows for the differentiation of solute source. Whereas comparison with pathfinder minerals potentially

indicates an association between metalloid concentrations with differing mineral or lithology endmembers. Surface waters are more variable, ranging from $^{87}Sr/^{86}Sr = 0.70750$ to 0.71331, compared to the groundwaters with values between 0.70682 to 0.70792 (Fig. 10A). Least radiogenic groundwaters have the highest Cu and Mo concentrations (Fig. 10C and D) and highest Rb/Sr values (Fig. 10A), whereas the most radiogenic surface waters have the lowest metals, Rb/Sr and Na/Cl (Fig. 10A and B).

Spatial distribution of stream water chemistry

Establishing background concentrations for the stream waters is complicated by the abundance of mineralized occurrences in the area (Fig. 2A). Due to the small dataset available, a simple statistical approach was used. The 90th percentile for each element was calculated, representing the concentration for which 90% of the data falls below. Background concentrations the pathfinder elements As (1.2 µg/L), Cd (0.06 µg/L), Co (0.38 µg/L), Cu (6.6 µg/L), Mo (1.1 µg/L), Re (0.02 µg/L), and Zn (3.6 µg/L), are close to the threshold values. The spatial distribution of stream and groundwater sample sites are shown in Appendix C map 1. Proportional dot maps of major and trace elements in stream water samples are shown in Appendix C maps 2 to 16. Regionally, many of the streams display concentrations considered background, including Excelsior, Britannia, Hayes, Colorado, and Sunshine creeks.

Casino Creek flows down-gradient from the western side of the deposit where weathering is shallowest and the main economic ore zones reside (Fig. 11). Casino Creek stream waters have elevated concentrations of Cd, Co, Cu, Mn, Mo, Pb, Re, U and Zn (Appendix C maps 5 and 9 to 15) up to 14 km downstream of the deposit. Surface waters around the Casino deposit are not anomalous in sulfate concentrations; the highest surface water sulfate concentrations occur in streams to the north of the Casino area (Appendix C map 8). However, sites 115J2017-1008, 115J2017-1010, and 115J2017-1014 close to the Casino deposit have the lowest $\delta^{34}S$ values of the surface waters, approaching the values observed in the metal- and sulfate-rich groundwaters from the deposit. Iron concentrations are elevated in stream waters of Casino Creek (Appendix C, map 4), ranging from 0.01 to 0.07 mg/L compared to a dataset median of 0.01 mg/L. The highest Fe concentrations (>0.2 mg/L) occur in sites 115J2017-1004 and 1005 (Hayes Creek), draining into the Selwyn River, and site 115J2017-1009, located in an unnamed tributary of Dip Creek. Similarly, Mn concentrations in Casino Creek are elevated, ranging from 35 to 104 µg/L (Appendix C, map 5), as well as site 115J2017-1009 (79 µg/L). Elsewhere in the district, Mn concentrations are generally below the dataset median of 5 µg/L.

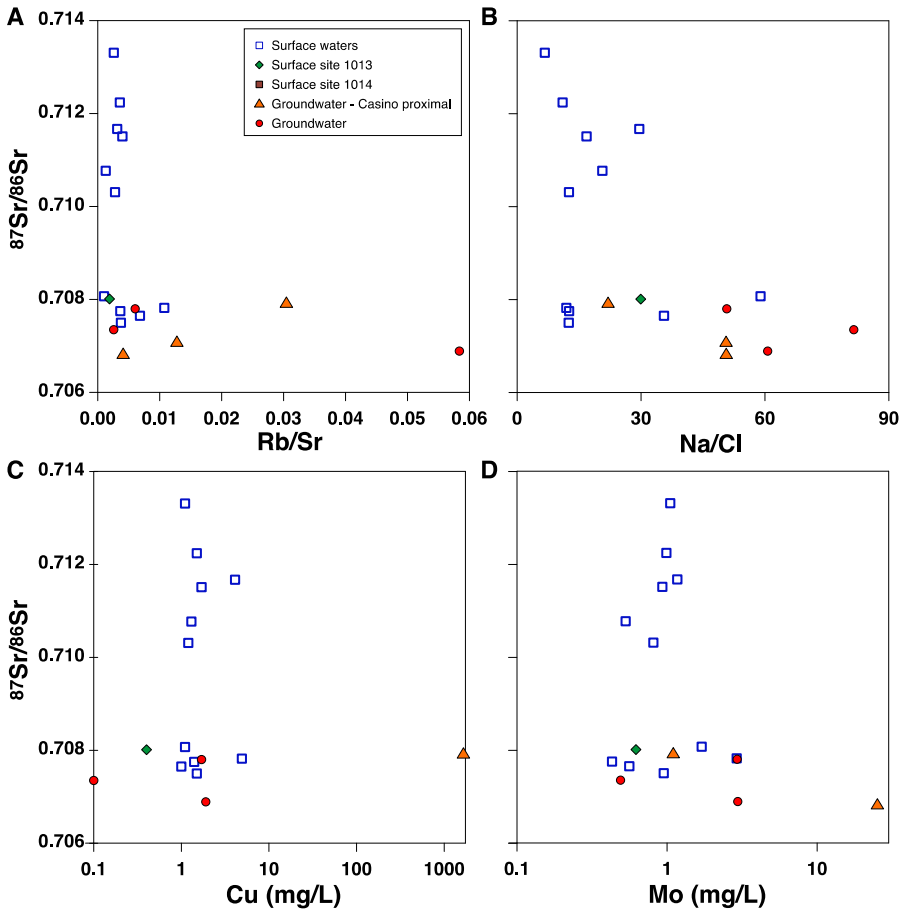

Figure 10. Strontium isotope ratios in Casino surface and groundwaters compared to A) Rb/Sr; B) Na/Cl; C) Cu (µg/L); and D) Mo (µg/L).

There is only a single stream water sample within 5 km of the deposit (Appendix C map 1), located within the Canadian Creek, which flows from the east of the deposit down-gradient to the north. Supergene weathering extends beyond a depth of 150 m in this zone and characterised by quartz-tourmaline and phyllic alteration suites (Roth et al., 2020). The major element chemistry of Canadian Creek is similar to those of Casino Creek, with Ca-SO_4^{2-} type waters, however; concentrations of dissolved trace elements are generally less than 10 µg/L.

Regionally, Ca concentrations in stream waters display a lithological control. Concentrations in excess of 40 mg/L (median 38 mg/L) appear to be associated with a Neoproterozoic and Paleozoic-aged Snowcap assemblage (Ryan et al., 2013), composed of quartzite, mica schist, and metaconglomerate (Appendix C map 6). Generally, there doesn't appear to be a spatial correlation between Ca concentration and mineralised occurrences in the district. Concentrations of NO_3 range from 1.22 to 1.91 mg/L (dataset median 1.2 mg/L) in Casino Creek (Appendix C map 7). The highest concentrations were

observed at sites 115J2017-1008 and 115J2017-1010, at the intersection of the Meloy and Casino Creek. Anomalous concentrations more than 1.5 mg/L are also present in Mascot Creek, downstream of the Mascot Au-Ag-As prospect, and in Isaac Creek, downstream of the Buck Au-As-Sb-Hg-Ba prospect. Site 115J2017-1002, about 20 km east of the Casino deposit, shows moderately anomalous Cd and Cu concentrations, and the highest Mo concentrations (2.91 µg/L) of all the surface waters in this study. This site is downstream from the Cockfield porphyry Cu-Mo-Au occurrence.

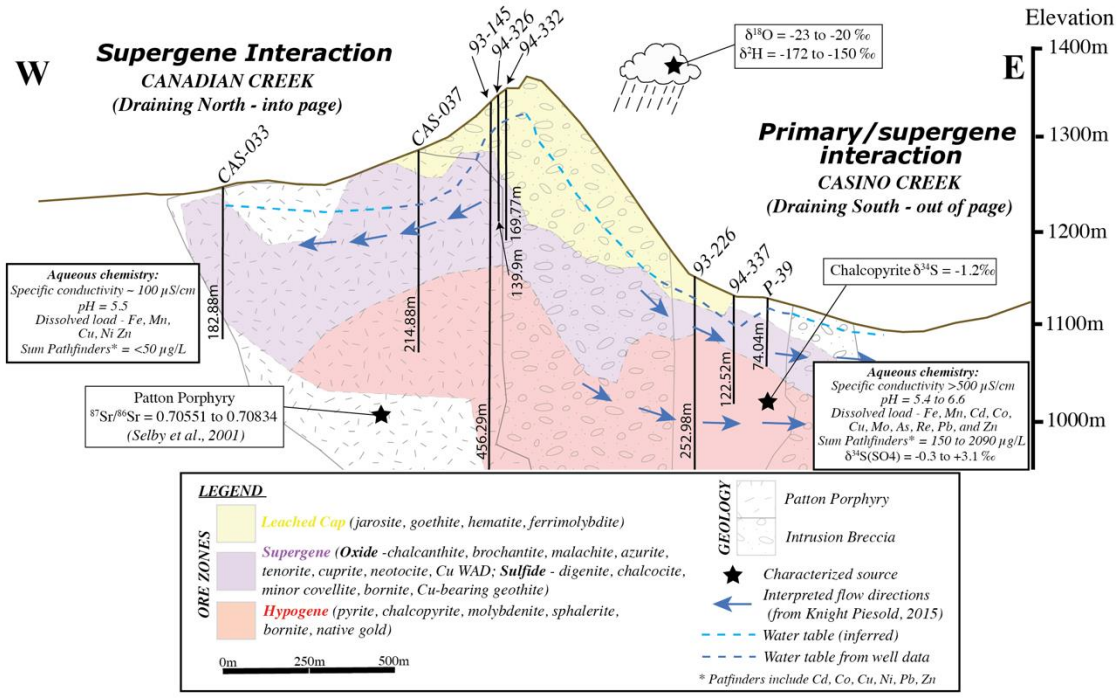

Figure 11. A conceptual model with east-west section with deposit mineralogy, host geology and hydrology.

DISCUSSION

Water provenance and sources of solutes

Stable isotope data for the surface and groundwater samples, show a tight clustering of $\delta^{18}O_{VSMOW}$ and $\delta^{2}H_{VSMOW}$ values around the mean annual weighted average for the precipitation monitoring stations in Whitehorse and Mayo (Fig. 8A). The isotopic composition of the groundwaters indicate that these are modern meteoric recharge waters, consistent with the low salinities. There is a slight enrichment in $\delta^{2}H_{VSMOW}$ compared to $\delta^{18}O_{VSMOW}$, which could represent a fractionation during snow melt events (Leybourne et al., 2006). However, the clustering of the surface waters with the groundwaters (Fig. 9A and B) indicates that the surface waters represent shallow groundwater discharge, with

dampened seasonal fluctuations, rather than being influenced by seasonal precipitation (Leybourne et al., 2006). Further, regional deep groundwater discharge is estimated to contribute 0.08 m3/s of water along the upper 7 km of Casino Creek (Knight-Piesold Ltd, 2015); however, mini-piezometer water level and calculated vertical gradients indicate fluctuating interconnection between ground and surface waters, with upward gradients increasingly prevalent during Fall months (Knight-Piesold Ltd, 2015). The surface waters also have generally higher TDS values (ranging 74 to 1314 mg/L, median 250 mg/L) than is typical for crystalline rock terrains. For example, in this study the average TDS of the surface waters is 262 ± 136 mg/L; surface waters in the Bathurst Mining Camp, New Brunswick, average 43.0 ± 31 mg/L (n = 560) (Leybourne et al., 2003). However, there are several points of evidence that indicate that there is a significant solute contribution from water-rock interaction.

Around the Casino deposit, groundwaters and surface waters proximal to mineralization have relatively non-radiogenic $^{87}Sr/^{86}Sr$ values (0.706 to 0.708), whereas other surface waters are more radiogenic (Fig. 10A). The less radiogenic values for proximal waters in this study are similar to values of hydrothermal K-feldspar from the Casino, Mt Nansen and Cash plutons, that vary from 0.70551– 0.70834 (Selby et al., 2001). However, there is potential overlap with the magmatic $^{87}Sr/^{86}Sr$ composition of country rocks from the Dawson Range batholith and metamorphic rocks of the Yukon-Tanana terrane, which range 0.707 to 0.722 (average 0.709, n = 70) (Selby et al., 1999). Waters in the study area with the most radiogenic Sr isotope values also have the lowest Rb/Sr, Na/Cl, Cu and Mo values (Fig. 10A, B, C, D), most consistent with mixing between Sr derived by water-pluton/deposit interaction with Sr derived from precipitation.

Fluoride concentrations in groundwaters proximal to Casino range from 0.03 to 1.00 mg/L (median 0.39), which is at the lower end of the published ranges for mineral dissolution related to granitic and metamorphic rocks (0.2 to 10.3 mg/l; Brindha and Elango, 2011). However, compared to distal ground or surface waters, molar ratios of F/Cl are elevated proximal to Casino, suggesting water-rock interaction with rock forming minerals with the alteration suite. Halogen elements are commonly found as components in the alteration shells of porphyry deposits, occurring in the hydroxyl sites of hydrosilicate minerals (e.g., apatite, fluorite, biotite, and hornblende; Idrus, 2018). Selby and Nesbitt (2000) determined the chemical composition of biotite at Casino within both the magmatic host rock and secondary, hydrothermal phases, reporting a marked increase in the F and Cl concentrations in biotite from the potassic and phyllic alteration zones. The F concentrations in groundwaters proximal to Casino are also controlled by the chemistry of the waters, with the neutral to alkaline pH of the ground and surface waters in the study area likely favoring the solubility and mobility of F (Brindha and Elango, 2011).

Water-deposit interaction – sources of dissolved solutes characteristic of porphyry Cu deposits

The ground and surface waters proximal to the Casino deposit are differentiated by anomalous concentrations of Cd, Co, Cu, Mo, As, Re, Pb, and Zn (compared to background). There are several possible explanations for the circum-neutral to alkaline (ranging from 5.4 to 8.3, median 7.7) ground and surface waters proximal to Casino: (i) the waters are highly buffered from hydrolysis reactions with the surrounding country rocks (clay mineral formation); (ii) the exceptional preservation of Casino means the waters interact with leached capping material, containing limited primary sulfide minerals and anomalies are the product of ion desorption from clays as well as Fe and Mn hydroxides; (iii) metal anomalies are the result of water interaction with supergene, oxide, and secondary sulfate mineralization; or (iv) significant mixing with fresh recharge is taking place.

It is unlikely a single explanation can account for the variation observed at Casino. There is evidence of at least some sulfide mineral oxidation taking place with high SO_4^{2-}, Fe, and Mn concentrations in groundwaters samples proximal to Casino and surface water sample 115J17-1014 from Casino Creek and acid generation (pH values down to 5.4). Additionally, despite significant variability of sulfur isotope values between the ground and surface waters, there is evidence of solute inputs from the oxidation of the Casino sulfide minerals. Waters proximal to mineralization, however, have $\delta^{34}S$ values similar to hypogene porphyry mineralization, ranging from -0.3 to +3.1 ‰. With increasing distance from mineralization, sulfate concentrations decrease and $\delta^{34}S$ values increase (Fig. 9B). The $\delta^{34}S$ values of the surface waters are similar to atmospheric SO_4^{2-} (Fig. 9B), with waters close to the Casino deposit having lower $\delta^{34}S$ values because of oxidation of sulfide minerals. The deep weathering and preservation of supergene horizons prevalent at Casino, suggests this could either be subaqueous oxidation of sulfide primary minerals, as observed at the Stratmat Main Zone deposit (New Brunswich) (Leybourne et al., 2009), or the oxidation of supergene sulfides. The likely fate of redox elements in oxygenated circumneutral waters is the precipitation as hydroxide phases (e.g., $Fe(OH)_3$) (Kyser et al., 2015), which commonly results in the creation of a reaction surface. Most sampled wells are located on the southern edge of the Casino deposit, within the phyllic alteration footprint. Surface and ground waters around the Casino deposit are anomalous with respect to Cd, Co, Cu, Mo, As, Re, Pb, and Zn concentrations. This generally correlates to the Casino mineralisation, which includes disseminations of pyrite, chalcopyrite, molybdenite, along with trace sphalerite and bornite (Casselman and Brown, 2017).

Depth to primary sulfides varies across the deposit; with supergene and oxide mineralisation predominant up to 280 m (Casselman and Brown, 2017) in the western portion of the deposit to less than 70 m in the eastern portion (Fig. 11). The largest anomaly occurs in sample LI992155-3, a groundwater sample collected from within the western

edge of the deposit footprint and the phyllic alteration halo. The highest Cd, Co, Cu, Ni, Pb, and Zn, concentrations in groundwater, along with one of the lowest pH values (5.4) are observed in sample LI992155-3. Located in the west of the deposit (Appendix C map 1), this site combines shallow weathering, a water table of less than 10 m, and deep groundwater flow (Knight-Piesold Ltd, 2015), suggesting potential heightened water interaction with primary sulfides.

Comparatively, concentrations of oxyanion forming elements As, Mo, and Re in proximal groundwaters are anomalous. Sources of As, Sb, and Se are typically constrained to the structure of primary sulfides such as pyrite (Manceau et al., 2020) and are therefore likely to have been leached and remobilised from the upper portions of the deposit. In comparison, Mo-bearing sulfide minerals are reported to be unaffected by supergene processes at Casino (Casselman and Brown, 2017).

Typically, Mo concentrations in stream and groundwaters are low (Smedley et al., 2014), with average global surface waters estimated to be 0.5 µg/L Mo (Reimann and de Caritat, 1998). Similarly, Re is typically present at very low concentrations in both ground and surface waters, generally <1 µg/L (Leybourne and Cameron, 2008). At Casino, Mo concentrations in proximal groundwaters are elevated up to 18 µg/L, reflecting the limited salinity of the waters in the district. Whereas surface waters range from 5 to 37 ng/L and groundwater Re concentrations are up to 710 ng/L (Figs. 6 and 7). Comparably, groundwaters within and down-gradient of the Spence porphyry Cu deposit in the Atacama Desert of northern Chile have been shown to have up to 100's of µg/L Mo and 31,000 ng/L Re (Leybourne and Cameron, 2008). It is also worth noting other possible sources of Re in natural waters. River waters in India have Re concentrations that vary from ~ 0.1 to 23.2 ng/L, with contributions controlled by weathering of black shales, mafic-rock associated pyrite and, at higher Re/K values, elevated Re was attributed to anthropogenic contributions (Rahaman et al., 2012). Essentially identical ranges of Re (1.3 to 26 ng/L) were observed in groundwaters from the Nevada Test Site, attributed to dissolution of marine carbonate rocks (Hodge et al., 1996). Comparatively, the Sisson Sn-W-Mo deposit (New Brunswick) displays anomalous Mo concentrations, ranging from 0.10 to 7.54 µg/L, from samples collected proximal to the deposit and up to 1 km downstream (McClenaghan et al., 2015). Compared to the porphyry case studies, all dissolved Re concentrations at Sisson are below detection.

The major ion and trace metal and metalloid composition of the ground and surface waters around the Casino deposit are consistent with water-rock interaction with the deposit. The S isotopic compositions of waters proximal to the Casino deposit are consistent with this interpretation. Compared to other case studies (Leybourne and Cameron, 2006a, b, 2008)

dissolved anomalies are relatively low, which likely reflects the extent of supergene development and leached capping at Casino.

Implications for mineral exploration

This study represents a rare opportunity to assess the potential of both surface and groundwaters as vectors to mineralization. The results demonstrate that mineral dissolution and element dispersion occurs in both ground and surface waters. Stream water anomalies associated with hydrothermal deposits are of relatively low concentration in the highly meteoric waters in Yukon, and in most cases are discernible only due to trace analysis with ICP-MS. However, such analysis is now a mainstream technique in many commercial laboratories with costs reflecting that. Additionally, there are many benefits to sampling stream waters, including (i) the relative ease of sampling access without the use of drilled well; (ii) the abundance of sample sources in many parts of the Yukon; and (iii) the relatively low cost of undertaking a sampling campaign.

There have been few studies that have investigated the groundwater geochemical and isotopic signatures around porphyry Cu deposits; the most extensive have been around the large Spence deposit in the Atacama Desert of northern Chile (Cameron et al., 2002; Leybourne and Cameron, 2006a; 2007; Leybourne and Cameron, 2008; Leybourne et al., 2013). Around the Spence deposit, groundwaters (and overlying soils) are anomalous in porphyry Cu-related elements, in particular Re, Se, As, Mo and Cu. However, Cu is only anomalous in the immediate vicinity of the Spence deposit, whereas Re, Se, Mo and As are anomalous for several km down-flow because they complex as oxyanions and are mobile in the surficial oxygenated and alkaline conditions, whereas Cu speciates as a metal cation and is lost through adsorption to Fe and Mn oxyhydroxide surfaces (Leybourne and Cameron, 2006b, 2008). Groundwaters proximal to the Casino deposit have elevated Re, Mo, As, Zn, and Mn concentrations (Fig. 12) in comparison to background stream and groundwaters, but much lower than the saline waters encountered at the Spence deposit.

A better comparison is the Taurus porphyry Cu deposit (Kelley and Graham, 2021), 140 km to the north-west of Casino, where a combination of exceptional preservation due to a lack of glacial activity and a sulfide mineral leached cap extending to a depth of 50 m limits Cu and Mo concentrations proximal to the deposit. Instead, a large (9 km) hydrogeochemical anomaly, consisting of B, Co, Mn, Re, and SO_4^{2-}, was detected in stream waters of McCord Creek, which drains the deposit (Kelley and Graham, 2021).

At both Casino and Taurus, the much lower concentrations trace metal cations observed in both ground and surface waters likely reflects the unique preservation of leached cap, oxide, supergene, and hypogene horizons (Fig. 11) (Casselman and Brown, 2017; Kelley and Graham, 2021) and potentially indicates that the results of this study may not be typical of porphyry hydrogeochemistry in Canada. Compared to Taurus, the ground and stream

waters collected from Casino generally have lower salinity, higher pH, and lower concentration anomalies. This may reflect the deeper weathering and leached horizon at Casino and reduced ligand availability for complexing. In any case, hydrogeochemical anomalies proximal to the deposits represent significant contrasts compared to background.

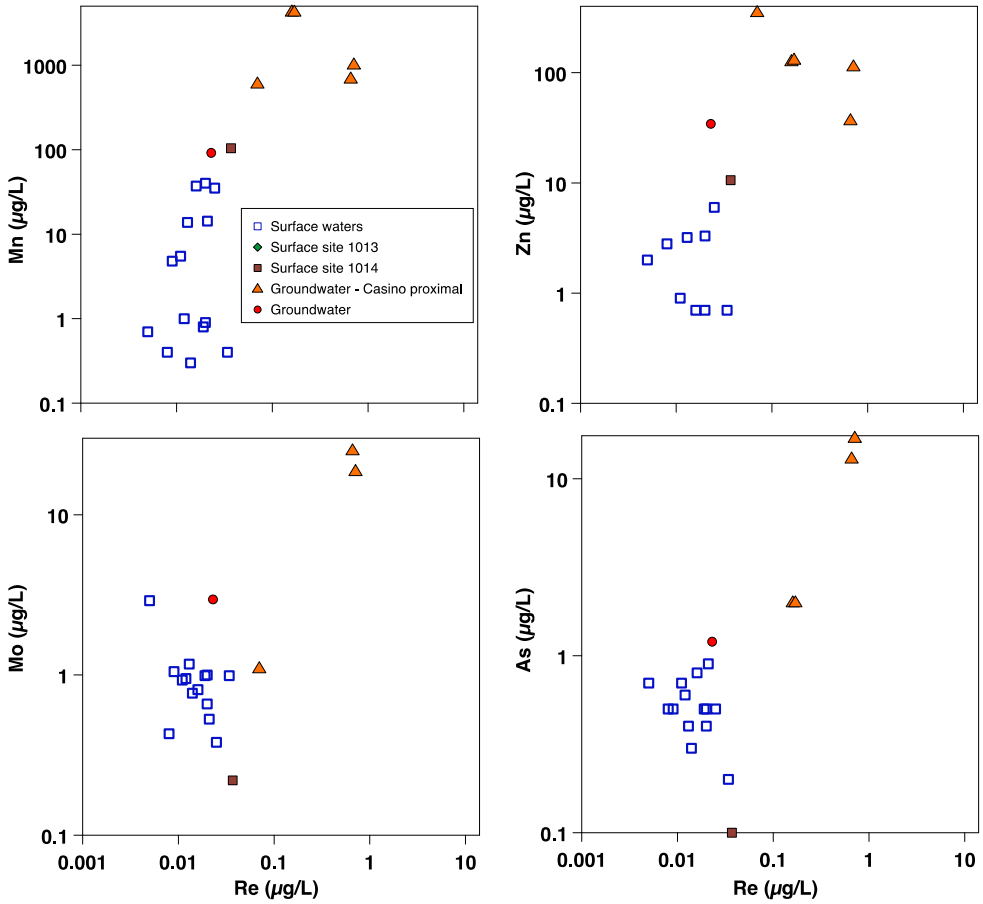

Figure 12. Metals and metalloids versus Re concentrations for Casino surface and groundwaters.

In all porphyry case studies (including Casino), Re is a notable pathfinder in surrounding waters. Rathkopf et al. (2017) noted that there are large variations in Re contents in molybdenite with total variation <15 to 4450 ppm in some 45 samples of 11 rock units at the Bagdad porphyry Cu-Mo deposit in Arizona, but variation of < 15 to 1215 ppm in a single molybdenite crystal. These authors noted that there was no systematic variation in Re contents of molybdenite as a function of lithology, degree of alteration, distance to ore, or ore grade, suggesting that Re contents of molybdenite may not be easily applied as a vector to porphyry Cu mineralization (Rathkopf et al., 2017). However, in aqueous systems, elevated Re may well prove an effective exploration tool, as shown here (Figs 6 and 7, Appendix C map 15) and in northern Chile (Leybourne and Cameron, 2008); i.e.,

the low background values for most ground and surface waters means that readily detectable Re in a water sample is likely anomalous. Groundwaters proximal to the Casino deposit have Re concentrations more than an order of magnitude higher than groundwaters from Nevada, for example (Hodge et al., 1996).

Surface waters at sites 115J2017-1008, 115J2017-1013 and 115J2017-1014 may be influenced by a pipe draining water from the Bomber prospect into the headwaters of Meloy Creek (Huss et al., 2013), upstream from site 115J2017-1013. However, Archer and Main (1971) collected surface waters and stream sediments in the area of the Casino deposit prior to any disturbance and reported Cu concentrations in creek waters that were anomalous compared to other streams in the area, with Cu values up to 2030 µg/L, only seen in groundwaters in this study. Archer and Main (1971) also reported that Taylor Creek (Fig. 3) had a flowing spring with a pH of 2.6 (much lower than any sample in this study) associated with a limonite gossan. Although they were unable to measure Mo in the waters, stream sediments were also anomalous in Mo (Archer and Main, 1971).

CONCLUSIONS

In this report, we have shown that the trace metal and metalloid composition of the surface and groundwaters close to the Casino porphyry Cu-Au-Mo deposit are consistent with water-deposit interaction and that hydrogeochemistry can be an effective exploration tool in this type of geological and morphological setting. Additional results from different isotope systems show that the ground and surface waters are meteoric, indicating recent recharge, and that deposit-water interaction is also reflected in the S and Sr isotopic compositions. Surface and ground waters around the Casino deposit are anomalous with respect to Cd, Co, Cu, Mo, As, Re, Pb, and Zn concentrations. In-particular Re, in addition to trace metal cations, appears to be an effective pathfinder in porphyry hydrogeochemical exploration.

Research is on-going, with additional sampling proposed to (i) test the effectiveness of Cu and Mo stable isotope measurements of dissolved phases as vectors to source; (ii) discriminate the signature of Casino and the Bomber occurrence; (iii) test the dispersion of metals in surface waters in dissolved and solid phases; and (iv) further confine the extent of the hydrogeochemical footprint, which is currently unconstrained. The results from additional research activities will be reported in subsequent publications.

ACKNOWLEDGEMENTS

This report is a contribution to Geological Survey of Canada's Targeted Geoscience Initiative Program (TGI-5). Support for this study was provided through the Porphyry-style Mineral Systems Project's 'Activity P-3.3: Mineralogical markers of fertility porphyry-style systems'. We gratefully acknowledge the support of Western Copper and Gold

Corporation and the Casino Mining Corporation, including access to the deposit and drill core and logistical support, in particular Mary Mioska and Heather Brown. Scott Casselman and Jeff Bond, Yukon Geological Survey, are thanked for sharing geological information, bedrock samples, and advice about the geology of the Casino area. This report benefited from a GSC review by Dr. Alexandre Desbarats.

REFERENCES

Allan, M., Mortensen, J., Hart, C., Bailey, L., Sanchez, M., Ciolkiewicz, W., McKenzie, G., Creaser, R., Colpron, M., and Bissig, T., 2013. Magmatic and metallogenic framework of west-central Yukon and eastern Alaska. Tectonics, Metallogeny, and Discovery: The North American Cordillera and Similar Accretionary Settings; Society of Economic Geologists, Special Publication 17, p. 111-168.

Archer, A., and Main, C., 1971. Casino, Yukon - a geochemical discovery of an unglaciated Arizona-type porphyry; *in* Geochemical Exploration, Proceedings of the 3rd International Geochemical Exploration Symposium, (ed.) R.W. Boyle; Canadian Institute of Mining and Metallurgy, p. 77.

Beckett-Brown, C.E., McDonald, A.M., and Mcclenaghan, M.B., 2019. Unravelling tourmaline in mineralized porphyry systems: assessment as a valid indicator mineral; *in* Targeted Geoscience Initiative: 2018 report of activities, (ed.) N. Rogers; Geological Survey of Canada, Open File 8549, p. 345-351, doi: https://doi.org/10.4095/313623.

Bond, J.D. and Sanborn, P.T., 2006. Morphology and geochemistry of soils formed on colluviated weathered bedrock: Case studies from unglaciated upland slopes in west-central Yukon; Yukon Geological Survey, Open File 2006-19, p. 70.

Bond, J.D., Lipovsky, P.S., MacFarlane, K., Weston, L., and Relf, C., 2010. Surficial geology, soils and permafrost of the northern Dawson Range; Yukon exploration and geology, p. 19-32.

Bond, J.D. and Lipovsky, P., 2012. Surficial geology of Colorado Creek (NTS115J/10) Yukon; Yukon Geological Survey, Open File 2012-2.

Bostock, H.S., 1959. Yukon Territory; *in* Tungsten deposits of Canada, (ed.) H.W. Little, Ottawa; Geological Survey of Canada, ser. 17

Bower, B., Payne, J., DeLong, C., Rebagliati, C., and Schroeter, T., 1995. The oxide-gold, supergene and hypogene zones at the Casino gold-copper-molybdenum deposit, west central Yukon; *in* Porphyry Copper Deposits of the Northwestern Cordillera of North America; Canadian Institute of Mining and Metallurgy and Petroleum, Montreal, Quebec, Special volume 46, p. 352-366.

Boyle, R., Hornbrook, E., Allan, R., Dyck, W., Smith, A. 1971. Hydrogeochemistry methods-application in the Canadian Shield; Geochemical exploration in the Canadian

Shield, State of the art-water, Canadian Institute of Mining, Metallurgy and Petroleum, Bull. 64, no. 715, p. 60-71.

Brindha, K. and Elango, L., 2011. Fluoride in groundwater: causes, implications and mitigation measures; *in* Fluoride properties, applications and environmental management, (ed.) S.D. Monroy, p. 111-136.

Buskard, J., Reid, N., and Gray, D., 2020. Parts per trillion (ppt) gold in groundwater: can we believe it, what is anomalous and how do we use it?; Geochemistry: Exploration, Environment, Analysis, v. 20, no. 2, p. 189-19.

Cameron, E.M., 1978. Hydrogeochemical methods for base metal exploration in the northern Canadian shield; Journal of Geochemical Exploration, v. 10, p. 219-243

Cameron, E.M., Leybourne, M.I., and Kelley, D.L., 2002. Exploring for deeply covered mineral deposits: Formation of geochemical anomalies in northern Chile by earthquake-induced surface flooding of mineralized groundwaters; Geology, v. 30, no. 11, p. 1007-1010.

Geological Survey of Canada, 1987. Regional stream sediment and water geochemical reconnaissance data, Yukon (NTS 115J, 115K (E1/2)); Geological Survey of Canada, Open File 1363, p. 142 pages, 1 diskette, doi: https://doi.org/10.4095/130284.

Casselman, S. and Brown, H., 2017. Casino porphyry copper-gold-molybdenum deposit, central Yukon (Yukon MINFILE 115J 028); Yukon Exploration and Geology Overview, p. 61-74.

Chapman, R., Allan, M., Grimshaw, M., Mortensen, J., Wrighton, T., and Casselman, S., 2014. Pathfinder signatures in placer gold derived from Au-bearing porphyries; Yukon Exploration and Geology, p. 21-31.

Clark, I.D. and Fritz, P., 1997. Environmental isotopes in hydrogeology, CRC Press, Boca Raton, New York, 1st Edition, p. 342.

Colpron, M., Israel, S., Murphy, D., Pigage, L., and Moynihan, D., 2016. Yukon bedrock geology map; Yukon Geological Survey, Open File 2016-1, scale 1:1 000 000.

Colpron, M., Nelson, J., and Murphy, D.C., 2006. A tectonostratigraphic framework for the pericratonic terranes of the northern Canadian Cordillera. Paleozoic evolution and metallogeny of pericratonic terranes at the ancient Pacific margin of North America, Canadian and Alaskan Cordillera; Geological Association of Canada Special Paper 45, p. 1-23.

Western Copper and Gold Corporation, 2020. Western Copper and Gold announces significant resource increase at Casino. <https://www.prnewswire.com/news-releases/western-copper-and-gold-announces-significant-resource-increase-at-casino-301092683.html> [accessed June 10, 2021].

Craig, H., 1961. Isotopic variations in meteoric waters; Science, v.133, pt. 3465, p. 1702-1703.

Day, S.J.A., Wodicka, N., and McMartin, I., 2013. Preliminary geochemical, mineralogical and indicator mineral data for heavy mineral concentrates and waters, Lorillard River area Nunavut (parts of NTS 56-A, -B, and -G); Geological Survey of Canada, Open File 7428, p. 11.

Duk-Rodkin, A., 2001. Glacial limits of Stevenson Ridge, Yukon Territory (115J&K); Geological Survey of Canada, Open File 3804, scale l:250,000. https://doi.org/10.4095/212275.

Duk-Rodkin, A., Weber, F., and Barendregt, R.W., 2002. Glacial limits of Upper Yukon River; Geological Survey of Canada, Open File 4275, scale 1:1000 000.

Duk-Rodkin, A., Barendregt, R.W., Froese, D.G., Weber, F., Enkin, R., Smith, I.R., Zazula, G.D., Waters, P., and Klassen, R., 2004. Timing and extent of Plio-Pleistocene glaciations in north-western Canada and east-central Alaska; Developments in Quaternary Sciences, v. 2, pt. B, p. 313-345.

Godwin, C.I. (1975) Geology of Casino porphyry copper-molybdenum deposit, Dawson Range, YT; Ph.D. thesis, University of British Columbia, Vancouver, https://open.library.ubc.ca/collections/ubctheses/831/items/1.0052877

Godwin, C.I., (1976) Casino; *in* Porphyry Deposits of the Canadian Cordillera: A Volume Dedicated to Charles S. Ney, (ed.) A.S. Brown; Canadian Institute of Mining & Metallurgy, Special volume 15.

Gromet, L.P., Dymek, R.F., Haskin, L.A., and Korotev, R.L., 1984. The "North American shale composite": its compilation, major and trace element characteristics; Geochim. Cosmochim. Acta, v. 48, p. 2469-2482.

Hall, G.E.M., Vaive, J.E., and McConnell, J.W., 1995. Development and application of a sensitive and rapid analytical method to determine the rare-earth elements in surface waters; Chemical Geology, v. 120, p. 91-109.

Hall, G.E.M., Vaive, J.E., and Pelchat, J-C., 1996. Performance of inductively coupled plasma mass spectrometric methods used in the determination of trace elements in surface waters in hydrogeochemical surveys; Journal of Analytical Atomic Spectrometry, v. 11, p. 779-786.

Hodge, V.F., Johannesson, K.H., and Stetzenbach, K.J., 1996. Rhenium, molybdenum, and uranium in groundwater from the southern Great Basin, USA: evidence for conservative behaviour; Geochimica et Cosmochimica Acta, v. 60, p. 3197-3214.

Huscroft, C.A., 2002a. Surficial geology, Britannia Creek, Yukon Territory (115J/15); Geological Survey of Canada, Open File 4345, scale 1:50 000, https://doi.org/10.4095/213868

Huscroft, C.A., 2002b. Surficial geology, Coffee Creek, Yukon Territory (115J/14); Geological Survey of Canada, Open File 4344, scale 1:50 000, https://doi.org/10.4095/213867.

Huscroft, C.A., 2002c. Surficial geology, Cripple Creek, Yukon Territory (115J/16); Geological Survey of Canada, Open File 4346, scale 1:50 000, https://doi.org/10.4095/213869

Huss, C., Drielick, T., Austin, J., Giroux, G., Casselman, S., Greenway, G., Hester, M., and Duke, J., 2013. Casino Project: Form 43-101F1 Technical report feasibility study; M3 Engineering & Technology Corporation, prepared for Western Copper and Gold, p. 205.

Idrus, A., 2018. Halogen chemistry of hydrothermal micas: a possible geochemical tool in vectoring to ore for porphyry copper-gold deposit; Journal of Geoscience, Engineering, Environment, and Technology, v. 3, p. 30-38.

Kelley, K.D., and Graham, G.E., 2021. Hydrogeochemistry in the Yukon-Tanana upland region of east-central Alaska: Possible exploration tool for porphyry-style deposits; Applied Geochemistry, v. 124, doi: https://doi.org/10.1016/j.apgeochem.2020.104821

Kidder, J., Voinot, A., Leybourne, M., Layton-Matthews, D., and Bowell, R., 2021. Using stable isotopes of Cu, Mo, S, and $^{87}Sr/^{86}Sr$ in hydrogeochemical mineral exploration as tracers of porphyry and exotic copper deposits; Applied Geochemistry, v. 128, doi: https://doi.org/10.1016/j.apgeochem.2021.104935.

Knight-Piesold Ltd. (2015) Casino Mining Corporation Casino Project - 2013-2014 Groundwater Data Report; Prepared for Casino Mining Corporation, v. VA101-325/17-1

Kyser, K., Barr, J., and Ihlenfeld, C., 2015. Applied geochemistry in mineral exploration and mining; Elements, v. 11, p. 241-246.

Leybourne, M.I., 2007. Aqueous geochemistry in mineral exploration; *in* Mineral Resources of Canada: A Synthesis of Major Deposit-types, District Metallogeny, the Evolution of Geological Provinces, and Exploration Methods, (ed.) W.D. Goodfellow, p. 1007-1034.

Leybourne, M.I., Boyle, D.R., and Goodfellow, W.D., 2003. Interpretation of stream water and sediment geochemistry in the Bathurst Mining Camp, New Brunswick: Applications to mineral exploration; *in* Massive Sulphide Deposits of the Bathurst Mining Camp, New Brunswick, and Northern Maine, (ed.) W.D. Goodfellow, S.R. McCutcheon, and S.R., Peter; Society of Economic Geologists, p. 741-762.

Leybourne, M.I., and Cameron, E.M., 2006a. Composition of groundwaters associated with porphyry-Cu deposits, Atacama Desert, Chile: Elemental and isotopic constraints on water sources and water-rock reactions; Geochimica et Cosmochimica Acta, v. 70, p. 1616-1635.

Leybourne, M.I., and Cameron, E.M., 2006b. Composition of soils and groundwaters at the Pampa del Tamarugal, Chile: anatomy of a fossil geochemical anomaly derived from a distant porphyry copper deposit; Economic Geology, v. 101, p. 1569-1581.

Leybourne, M.I., and Cameron, E.M., 2008. Source, transport, and fate of rhenium, selenium, molybdenum, arsenic, and copper in groundwater associated with porphyry-Cu deposits, Atacama Desert, Chile; Chemical Geology, v. 247, p. 208-228.

Leybourne, M., and Cameron, E.M., 2010. Groundwater in geochemical exploration; Geochemistry: Exploration, Environment, Analysis, v. 10, p. 99-118.

Leybourne, M.I., Cameron, E.M., Reich, M., Palacios, C., Faure, K., and Johannesson, K.H., 2013. Stable isotopic composition of soil calcite (O, C) and gypsum (S) overlying Cu deposits in the Atacama Desert, Chile: Implications for mineral exploration, salt sources, and paleoenvironmental reconstruction; Applied Geochemistry, v. 29, p. 55-72.

Leybourne, M.I., Clark, I.D., and Goodfellow, W.D., 2006. Stable isotope geochemistry of ground and surface waters associated with undisturbed massive sulfide deposits: constraints on origin and water-rock reactions; Chemical Geology, v. 231, p. 300-325.

Leybourne, M.I., and Cousens, B.L., 2005. Rare earth elements (REE) and Nd and Sr isotopes in groundwater and suspended sediments from the Bathurst Mining Camp, New Brunswick: water-rock reactions and elemental fractionation; *in* Rare Earth Elements in Groundwater Flow Systems, Water Science and Technology Library, (ed.) K.H. Johannesson, Springer, Dordrecht, v. 51, p. 254-293.

Leybourne, M.I., Cousens, B.L., and Goodfellow, W.D., 2009. Lead isotopes in ground and surface waters: fingerprinting heavy metal sources in mineral exploration; Geochemistry: Exploration, Environment, Analysis, v. 9, p. 115-123.

Lipovsky, P.S., and Bond, J.D., 2012. Surficial geology of Doyle Creek (115J/11), Yukon; Yukon Geological Survey, Open File 2012-3.

Manceau, A., Merkulova, M., Mathon, O., Glatzel, P., Murdzek, M., Batanova, V., Simionovici, A., Steinmann, S.N., and Paktunc, D., 2020. The mode of incorporation of As (-I) and Se (-I) in natural pyrite revisited; ACS Earth and Space Chemistry, v. 4, p. 379-390.

Mathur, R., Ruiz, J., Titley, S., Liermann, L., Buss, H., and Brantley, S., 2005. Cu isotopic fractionation in the supergene environment with and without bacteria; Geochimica et Cosmochimica Acta, v. 69, p. 5233-5246.

Mathur, R., Titley, S.R., Schlitt, W.J., and Wilson, M., 2012. Cu isotope fractionation in exploration geology and hydrometallurgy: examples from porphyry copper deposits; Mining Engineering, v. 64, p. 42-46.

Mathur, R., Munk, L., Nguyen, M., Gregory, M., Annell, H., and Lang, J., 2013. Modern and Paleofluid Pathways Revealed by Cu Isotope Compositions in Surface Waters and

Ores of the Pebble Porphyry Cu-Au-Mo Deposit, Alaska; Economic Geology, v. 108, p. 529-541.

McArthur, J.M., 1994. Recent trends in strontium isotope stratigraphy; Terra Nova, v. 6, p. 331-358.

McClenaghan, M.B., and Paulen, R.C., 2018. Application of till mineralogy and geochemistry to mineral exploration; Chapter 20 *in* Past glacial environments (second edition), (ed.) J. Menzies and Jaap J.M. van der Meer, Elsevier, p. 689-751.

McClenaghan, M.B., 2005. Indicator mineral methods in mineral exploration; Geochemistry: Exploration, Environment, Analysis, v. 5, p. 233-245.

McClenaghan, M.B., Beckett-Brown, C.E., McCurdy, M.W., McDonald, A.M., Leybourne, M.I., Chapman, J.B., Plouffe, A., and Ferbey, T., 2018. Mineral markers of porphyry Cu mineralization: Progress report on the evaluation of tourmaline as an indicator mineral; *in* Targeted Geoscience Initiative: 2017 Report of Activities, (ed.) N. Rogers; Geological Survey of Canada, Open File 8358, p. 69-77. doi: https://doi.org/10.4095/306427.

McClenaghan, M.B., McCurdy, M.W., Beckett-Brown, C.E., and Casselman, S.C., 2020. Indicator mineral signatures of the Casino porphyry Cu-Au-Mo deposit, Yukon; Geological Survey of Canada, Open File 8711, p. 42.

McClenaghan, M.B., McCurdy, M.W., Garrett, R.G., Beckett-Brown, C.E., Leybourne, M.I., Casselman, S.G., and Pelchat, P., 2019. Mineral and geochemical signatures of porphyry copper mineralization: work in progress for the Casino Cu-Au-Mo-Ag porphyry deposit, Yukon; *in* Targeted Geoscience Initiative: 2018 report of activities, (ed.) N. Rogers; Geological Survey of Canada, Open File 8549, p. 333-344. doi: https://doi.org/10.4095/313623.

McClenaghan, M.B., Parkhill, M.A., Pronk, A.G., McCurdy, M.W., Boldon, G.R., Leyboume, M.I., Pyne, R.M., and Rice, J.M., 2015. Geochemical and indicator mineral data for stream sediments and waters around the Sisson Sn-W-Mo deposit, New Brunswick (NTS 21-J/06, 21-J/07); Geological Survey of Canada, Open File 7756, p. 62, doi: https://doi.org/10.4095/297246.

McCurdy, M.W., Mcclenaghan, M.B., Garrett, R.G., and Pelchat, P., 2019. Geochemical signatures of the silt fraction from streams near the Casino porphyry Cu-Au-Mo deposit, Yukon Territory; Geological Survey of Canada, Open File 8632.

McCurdy, M.W., and McNeil, R.J., 2014. Geochemical data from stream silts and surface waters in the Pine Point mining district, Northwest Territories (NTS 85-B); Geological Survey of Canada, Open File 7577. doi: https://doi.org/10.4095/293913.

McDonough, W.F., and Sun, S.S., 1995. The composition of the Earth; Chemical Geology, v. 120, p. 223-253.

McKillop, R., Turner, D., Johnston, K., and Bond, J., 2013. Property-scale classification of surficial geology for soil geochemical sampling in the unglaciated Klondike Plateau, west-central Yukon; Yukon Geological Survey, Open File 2013-15.

McLennan, S.M., 1989. Rare earth elements in sedimentary rocks: influence of provenance and sedimentary processes; Reviews in Mineralogy and Geochemistry, v. 21, p. 169-200.

Moran, K., Backman, J., Brinkhuis, H., Clemens, S.C., Cronin, T., Dickens, G.R., Eynaud, F., Gattacceca, J., Jakobsson, M., and Jordan, R.W., 2006. The cenozoic palaeoenvironment of the arctic ocean; Nature, v. 441, p. 601-605.

Mortensen, J.K., and Friend, M., 2020. An overview of porphyry style deposits in Yukon, Porphyry Deposits of the Northwestern Cordillera of North America: A 25 Year Update; Canadian Institute of Mining and Metallurgy.

Nelson, J.L., Colpron, M., Piercey, S., Dusel-Bacon, C., Murphy, D., and Roots, C., 2006. Paleozoic tectonic and metallogenic evolution of the pericratonic rocks of east-central Alaska and adjacent Yukon Territory; Special Paper-Geological Association of Canada, v. 45, p. 25-74.

Nelson, J., Colpron, M., Israel, S., Bissig, T., Rusk, B., and Thompson, J., 2013. The cordillera of British Columbia, Yukon, and Alaska: tectonics and metallogeny; *in* Tectonics, Metallogeny, and Discovery: The North American Cordillera and Similar Accretionary Settings; Society of Economic Geologists, Special Publication 17, p. 53-109.

Rahaman, W., Singh, S.K., and Shukla, A.D., 2012. Rhenium in Indian rivers: Sources, fluxes, and contribution to oceanic budget; Geochemistry, Geophysics, Geosystems, v. 13, doi: https://doi.org/10.1029/2012GC004083

Rathkopf, C., Mazdab, F., Barton, I., and Barton, M.D., 2017. Grain-scale and deposit-scale heterogeneity of Re distribution in molybdenite at the Bagdad porphyry Cu-Mo deposit, Arizona; Journal of Geochemical Exploration, v. 178, p. 45-54.

Reimann, C., and de Caritat, P., 1998. Factsheets for the geochemist and environmental scientist; *in* Chemical elements in the environment; Springer, Belin, Heidelberg, p. 398.

Relf, C., 2020. Yukon Geological Survey: Planning for the future; *in* Yukon exploration and geology overview 2019, (ed.) K.E. Macfarlane; Yukon Geological Survey, p. 1-22.

Romaniello, S.J., Field, M.P., Smith, H.B., Gordon, G.W., Kim, M.H., and Anbar, A.D., 2015. Fully automated chromatographic purification of Sr and Ca for isotopic analysis; Journal of Analytical Atomic Spectrometry, v. 30, p. 1906-1912.

Roth, D., Hester, M., Tahija, L.M., Schulze, C., and Vallat, C.J., 2020. Casino Project: Form 43-101F1 Technical report mineral resource statement, Yukon, Canada; M3 Engineering & Technology Corporation, prepared for Western Copper and Gold, p. 150.

Ryan, J., Zagorevski, A., Williams, S., Root, C., Ciolkiewicz, W., and Chapman, J., 2013. Geology, Stevenson Ridge (northeast part), Yukon; Geological Survey of Canada, Canadian Geoscience Map 116 (preliminary), scale 1:100 000.

Selby, D., Creaser, R.A., and Nesbitt, B.E., 1999. Major and trace element compositions and Sr-Nd-Pb systematics of crystalline rocks from the Dawson Range, Yukon, Canada; Canadian Journal of Earth Sciences, v. 36, p. 1463-1481.

Selby, D., and Nesbitt, B.E., 2000. Chemical composition of biotite from the Casino porphyry Cu–Au–Mo mineralization, Yukon, Canada: evaluation of magmatic and hydrothermal fluid chemistry; Chemical Geology, v. 171, p. 77-93.

Selby, D., Nesbitt, B.E., Creaser, R.A., Reynolds, P.H., and Muehlenbachs, K., 2001. Evidence for a nonmagmatic component in potassic hydrothermal fluids of porphyry cu-Au-Mo systems, Yukon, Canada; Geochimica et Cosmochimica Acta, v. 65, p. 571-587.

Skierszkan, E.K., Robertson, J.M., Lindsay, M.B., Stockwell, J.S., Dockrey, J.W., Das, S., Weis, D., Beckie, R.D., and Mayer, K.U., 2019. Tracing molybdenum attenuation in mining environments using molybdenum stable isotopes; Environmental science & technology, v. 53, p. 5678-5686.

Smedley, P.L., Cooper, D.M., Ander, E.L., Milne, C.J., and Lapworth, D.J., 2014. Occurrence of molybdenum in British surface water and groundwater: Distributions, controls and implications for water supply; Applied Geochemistry, v. 40, p. 144-154

Smet, I., De Muynck, D., Vanhaecke, F., and Elburg, M., 2010. From volcanic rock powder to Sr and Pb isotope ratios: a fit-for-purpose procedure for multi-collector ICP–mass spectrometric analysis; Journal of Analytical Atomic Spectrometry, v. 25, p. 1025-1032.

Smith, C., Meikle, J., and Roots, C., 2004. Ecoregions of the Yukon Territory: Biophysical properties of Yukon landscapes; Agriculture and Agri-Food Canada, PARC Technical Bulletin No. 04-01, Summerland, British Columbia, p. 313.

Thorleifson, L.H., 2017. History and status of till geochemical and indicator mineral methods in mineral exploration; *in* New frontiers for exploration in glaciated terrain, (ed.) R.C. Paulen and M.B. McClenaghan, Geological Survey of Canada, Open File 7374, p. 1-5.

Vavrek, M.J., Evans, D.C., Braman, D.R., Campione, N.E., and Zazula, G.D., 2012. A Paleogene flora from the upper Bonnet Plume formation of northeast Yukon Territory, Canada; Canadian Journal of Earth Sciences, v. 49, p. 547-558.

Wang, L., Zhang, Y., Sun, N., Sun, W., Hu, Y., and Tang, H., 2019. Precipitation methods using calcium-containing ores for fluoride removal in wastewater; Minerals, v. 9, p. 511.

Yukon Geological Survey, 2020a. Buck occurrence. http://data.geology.gov.yk.ca/Occurrence/14418 (accessed January 24, 2020).

Yukon Geological Survey, 2020b. Marquerite occurence. http://data.geology.gov.yk.ca/Occurrence/14417 (accessed January 24, 2020).

Yukon Geological Survey, 2020c. Occurrence 115J 017. Cockfield occurrence. http://data.geology.gov.yk.ca/Occurrence/14367. (accessed January 24, 2020).

Yukon Geological Survey, 2020d. Occurrence 115J 023. Nordex occurrence. http://data.geology.gov.yk.ca/Occurrence/14372 (accessed January 24, 2020).

Yukon Geological Survey, 2020e. Occurrence 115J 027. Bomber occurrence. http://data.geology.gov.yk.ca/Occurrence/14376 (accessed January 24, 2020).

Yukon Geological Survey, 2020f. Occurrence 115J 028. Casino occurrence. http://data.geology.gov.yk.ca/Occurrence/15019 (January 24, 2020)

Yukon Geological Survey, 2020g. Occurrence 115J 036. Zappa occurrence. http://data.geology.gov.yk.ca/Occurrence/14384 (accessed January 24, 2020).

Yukon Geological Survey, 2020h. Occurrence 115J 074. Mascot occurrence. http://data.geology.gov.yk.ca/Occurrence/14421 (accessed January 24, 2020).

Yukon Geological Survey, 2020i. Occurrence 115J 099. Idaho occurrence. http://data.geology.gov.yk.ca/Occurrence/15100 (accessed January 24, 2020).

Yukon Geological Survey, 2020j. Occurrence 115J 101. Canadian Creek occurrence. http://data.geology.gov.yk.ca/Occurrence/14431 (accessed January 24, 2020).

Yukon Geological Survey, 2020k. Overview of Yukon geology. (accessed January 24, 2020).

Yukon Geological Survey, 2020l. Rude Creek occurrence. http://data.geology.gov.yk.ca/Occurrence/14371 (accessed January 24, 2020).

Yukon Geological Survey, 2020m. Yukon digital bedrock geology, http://www.geology.gov.yk.ca/update_yukon_bedrock_geology_map.html, (accessed January 24, 2020).

Zachos, J., Pagani, M., Sloan, L., Thomas, E., and Billups, K., 2001. Trends, rhythms, and aberrations in global climate 65 Ma to present; science, v. 292, p. 686-693.